Surficial morphology of Eastern Valley, Laurentian Fan.

J.E. Hughes Clarke

Department of Oceanography,

Dalhousie University,

Halifax, N.S., B3H 4J1

Geological Survey of Canada Open file Report # 1425

January, 1987.

This open file consists of a sidescan sonar mosaic at 1 : 200,000 of 500 km of SeaMARC I imagery of Eastern Valley, Laurentian Fan, extending from the 3000m isobath to the 5000m isobath, together with a short interpretive text and illustrations.

ABSTRACT

Eastern Valley, the major axial valley of the Laurentian Fan has been investigated using the SeaMARC I sidescan system. The sidescan images, together with complementary reflection profiles are used to describe the surficial morphology of the valley.

The floor and margins of Eastern Valley display a unique set of erosional and depositional features that resulted from the passage of a large turbidity current following the 1929 Grand Banks earthquake. Gravel wavefields occur on elevated regions of the valley floor, whereas sand deposits lie in bathymetric lows and channels entrenched within the floor. The valley margins in contrast have been eroded by flow such that Pleistocene sediment is exposed at the seafloor. Long wavelength sand bedforms occur on the proximal depositional lobe south of lower Eastern Valley.

INTRODUCTION

Interest in the drainage of the Laurentian Fan began as a result of investigations into the cable breaks following the 1929 Grand Banks earthquake (Heezen and Ewing, 1952). Instantaneous cable breaks throughout the upper fan suggest that widespread failure of slope sediments took place (Fig. 1). Delayed cable breaks suggest that turbidity currents propagated downslope with head velocities of 10 to 20 m/s (Heezen and Ewing, 1952, Menard, 1964).

In 1980 a series of large scars were recognised on GLORIA images of the upper slope close to the epicentre of the 1929 earthquake (Masson et al., 1985). As a result SeaMARC I was deployed in 1983 (Fig. 3, Hudson 83-017) to observe in more detail the effect of the earthquake. Images obtained in 1983 revealed considerable modification of the upper slope in the epicentral region that could be attributed to the 1929 earthquake (Piper et al., 1985). In the head of Eastern Valley, close to the epicentre, gravel waves and elongate sand ribbons were imaged on the valley floor suggesting recent modification of the floor by traction flow (Piper et al., 1985). The aim of the 1984 SeaMARC survey (Fig. 3, Hudson

84-040) was to establish the extent and development of these features along the valley.

The regional drainage pattern of upper and middle Laurentian Fan is best defined from GLORIA imagery (Masson et al., 1985, fig. 5). There are two major axial drainage features, Eastern and Western Valleys (Fig. 2). Eastern Valley is the largest drainage feature on the Laurentian Fan and can be traced across the rise to the 5000m contour. Eastern Valley is not fed by shelf-breaching canyons. The head of Eastern Valley lies on the upper slope between Laurentian Channel and St. Pierre Bank. A major tributary, Grand Banks Valley, drains the slope below Haddock and Halibut Channels (Fig. 2). Eastern and Grand Banks Valleys merge at 43°30'N at a depth of 4100m.

The upper (<2000m) and middle (2000 to 4500m) sections of Eastern Valley are straight, with a 20 to 25 km wide floor. The west wall of the valley is elevated up to 900m above the valley floor. The east wall of the valley is more subdued with a maximum elevation of 300m. South of 43°00'N, Eastern Valley divides into two branches, here refered to as East and South Branches, separated by the Interbranch High. The upper and middle valley drains to the SSE. East and South Branches together make up lower Eastern Valley which drains to the SE. East Branch has a low sinuosity, curving gently from SSE to SE with a 5 to 7 km wide floor. South Branch in contrast becomes sinuous and partially entrenched, before turning to the SE onto a depositional fan lobe. The proximal region of the lobe immediately to the SE of the lower valley branches is termed here the Valley Termination Zone.

In October 1984 (Hudson 84-040), 500 line km of SeaMARC I sidescan and subbottom were obtained along with 12 kHz, 3.5 kHz and 40 cu. in. airgun profiles. There were two SeaMARC deployments in Eastern Valley (Fig. 3). The first deployment (310 line km) consisted of a zigzag reconnaisance survey along the axis of Eastern Valley. This deployment began in 3000m water depth in the middle valley floor and was terminated at 4600m water depth in South Branch. The second deployment took place in 4800m of water within the Valley Termination Zone and consisted of 3 subparallel survey lines totalling 190 line km across the Valley Termination Zone and the end of South Branch.

Complementary, airgun reflection profiles, piston cores, bottom camera stations and

submersible dives were obtained on two subsequent cruises (Hudson 85-001, Pandora 85-059).

Previous cruise data discussed in this report include:

Hudson 73-011 (cores), (Stow 1977),

Hudson 73-031 (cores), (Stow 1977),

Hudson 74-021 (cores), (Stow 1977),

Discovery 111 (GLORIA images), (Masson et al., 1985),

Hudson 83-017 (SeaMARC images), (Piper et al., 1985),

Dawson 84-003 (cores), (Piper et al., 1984).

METHODS

SeaMARC 1 is a deeply towed sidescan sonar and subbottom profiler package (Kosalos and Chayes, 1983) capable of working to depths of 6000m. The sidescan has two transducer arrays, operating at 27 and 30 kHz respectively which can be operated in 1, 2 or 5km total swath width mode. The system has been developed to produce real-time, slant-range corrected, orthorectified images. The subbottom profiler system consists of a 4.5 kHz transducer. In the 5 km swath mode, the towfish is towed about 300 m off the bottom. The towfish is neutrally buoyant, isolated from surface ship motion by use of an umbilical cord behind a towed depressor weight. For the depths of water encountered on the survey (3000-5000m) the maximum tow velocity was less than 2 knots.

Navigation was by LORAN C with phase lag corrections empirically applied by comparison of LORAN C and satellite data. The position of the towbody was estimated with a knowledge of vehicle depth, surface wire angle and length of cable out. No acoustic ranging was employed.

The orthorectified sidescan images were manually compiled into a mosaic at a scale of 1:40,000. The mosaic has been divided into eleven sheets (Fig. 3) which have been photographically reproduced to a scale of 1:200,000 as Plates I-XI.

Bottom photography was undertaken with the BIO U-MEL deep camera system. On Hudson cruise 85-001, vertical stereo pairs were obtained with a trigger height of 8 ft. On Pandora cruise 85-059, the trigger height remained at 8 ft., but one of the cameras was mounted at

30 deg. to the vertical to obtain an oblique view of the seabed.

Submersible studies were carried out to a depth of 2000m in the epicentral region using Pisces IV (Fig.5), deployed from MV. Pandora II (Hughes Clarke et al., 1987). 27 hours of on bottom video from four dives were obtained. Shallow penetrating cores (< 30cm) and grab samples were taken from the submersible.

SEDIMENTS

A total of 20 bottom samples have been recovered in the last 35 years from the floors of the valleys of Laurentian Fan. Two cores have been recovered from Western Valley, fourteen cores and three grabs from Eastern Valley and one box core from Grand Banks Valley (Fig. 4 & 5, table 1). Pebbles and sand were recovered during cable repair work following the 1929 earthquake (Kindle, 1931) and Heezen, Ericson and Ewing (1954) recovered sand and gravel from cores in the valleys and on the lobe. A single box core containing sand and gravel was recovered from the Grand Banks Valley (Sanders, 1969). Cores containing normally graded well-sorted gravels were recovered from Western Valley and East Branch of Eastern Valley in 1973-4 (Stow, 1977). Recent coring (cruises 84-003, 84-040, 85-001, 85-059) has been focussed on Eastern Valley.

Pebbly mudstones outcrop on upper Eastern Valley floor. The pebbly mudstone is probably Pleistocene proximal glaciomarine sediment (Hughes Clarke et al., 1987). Till tongues have been recognised on the upper slope adjacent to the head of Eastern Valley (Meagher, 1984). These glacially derived sediments were probably formed during periods of ice advance when the Laurentian Channel was the major ice outlet on the Canadian east coast margin (Stow, 1977). In middle Eastern Valley, poor core recovery is common as a result of extremely coarse sediments. The largest clasts recovered in a piston core are about 5cm in size, whereas boulders larger than 2m at 2000m (Pisces dive 1640) and up to 50cm in size at 4300m (Camera stn. 1, 85-001) are known to exist. In lower Eastern Valley 7 piston cores have been recovered which penetrate betwen 125 and 580cm. The lower valley cores grade from a surface mud to gravel in the top 1m and consist of well sorted granule to pebble gravel thereafter.

Red semiconsolidated mud rip-up clasts are present in these cores (1-5cm) implying that Pleistocene sediment has been eroded from the valley margins.

There is no active mechanism today for supply of coarse sediment from the shelf into Eastern Valley. The pebbly mudstones in the upper valley, however, represent a potential source for the coarse sediment found in Eastern Valley. The lithologies of sediment clasts recovered from the valley floor include granites, metamorphic rocks, limestones and arenites, all derived from erosion of outcropping units on the Canadian eastern seaboard (Stow, 1977). The lithologic immaturity of the valley floor sediments reflects their derivation from a singly reworked glacial source rather than a multiply reworked shelf source. The gross downvalley trend of decreasing grain size and increased sorting reflects the increasing degree of transport undertaken by the sediment down the valley.

MORPHOLOGY

Valley floor channels

Channels are developed within the floor of middle Eastern Valley. The channels sit 50 to 100m below the main valley floor and are a few kilometres wide. The channels are most common adjacent to the valley walls. In one instance, a channel is located adjacent to a small intravalley high. Such channels are, however, absent from the narrower floors of South and East Branches. The channels are not continuous along the valley margins, but rather they deepen and shoal along the length of the valley without meandering.

The position of the valley-floor channels immediately adjacent to the valley walls or intravalley highs may imply increased secondary flow due to the presence of a lateral boundary. Such a mechanism was suggested for comparable marginal channels described adjacent to canyon walls through which the late Pleistocene Bonneville floods flowed (Malde, 1968). The Bonneville Flood channels are separated by bars of extremely coarse sediment (the Melon gravel) comparable in size to the sediment on the floor of Eastern Valley.

Gravel waves

Periodic transverse lineations on the valley floor, developed in sediment with high acoustic backscatter, were first recognised from SeaMARC images and interpreted as gravel wave bedforms by Piper et al. (1985). They attributed the presence of the bedforms to a turbidity current generated as a result of the 1929 Grand Banks earthquake.

These gravel waves first appear in 1500m water depth in upper Eastern Valley and dominate the middle valley floor. The gravel waves are asymmetric-dune type bedforms, oriented transverse to flow with sinuous elongate crests (Fig. 6a). The gravel waves occur in wavefields that cover up to 80% of the valley floor. The average gravel wavecrest spacing increases from 30m in 2000m water depth to 70m by 3500m and is between 40 and 80m on the valley floor deeper than 4000m. Acoustic shadows formed by the gravel wavecrests on SeaMARC images suggest the bedform amplitude is between 1 and 5m. Commonly the gravel waves occur in lanes of wave trains. The lanes are separated by either elongate zones of lower acoustic backscatter or compound zigzag junctures (Fig. 6a). On 4.5kHz subbottom records the gravel waves appear as discrete hyperbolic echos with a high amplitude surface reflection and no subbottom penetration (Fig. 10).

Poor core penetration (less than 1m) has been achieved within the gravel wavefields as a result of the large clast sizes present on the seafloor. As a result the internal structure of the bedforms is unknown. Two cores taken within a gravel wavefield (Fig. 7) produced coarse sand and large pebbles. The poor core penetration (70 and <15cm) and severe damage to the core cutters implied impact with coarser clasts. The poor sorting of these sediments may be a result of mixing of an originally graded thin surface layer, although both cores were too severely disturbed to see any structure. Piston cores taken from the floor of middle and lower Eastern Valley suggest that the upper surfaces of the gravel waves are draped by a normally graded gravel to mud deposit which thickens downvalley.

Observations from Pisces IV in 2000m water depth indicated that the gravel waves overlie eroded, semiconsolidated mudstone and pebbly mudstone outcrop (Dive 1640, Hughes Clarke et al., 1987). The gravel wavecrests are seen as a series of steps in the seafloor of 1 to 4m

amplitude, facing downslope. On the stoss sides cobbles and boulders are exposed through a mud draped seafloor. This seafloor is hard, consisting of a gravel pavement overlain by 2 to 10cm of mud. The mud drape is thickest over the lee slopes. Cobble and boulder lags are still seen in gravel wavefields at 4300m but are absent at 4600m (HN 85-001 camera station #2 and #4).

In the middle valley the largest gravel wavefields occur on areas of positive relief away from valley floor channels. In the lower valley the narrow floors of South and East Branches have a simple morphology with gravel waves largely restricted to the flanks of the floor on either side of central low (Fig. 10 & 11).

The only known analogous marine bedforms occur on the floor of Var canyon (Malinverno et al., 1987). These bedforms resulted from a recent (1979) slide starting from the end of Nice airport. Similar scale asymmetric dunes, constructed of gravel and boulders, exist in the Scablands of Washington State (the "Giant Ripples" of Bretz, 1956 and Baker, 1973). These bedforms were constructed during a Pleistocene catastrophic flood. Large-scale cross bedding and dunes have been described from resedimented conglomerates in ancient deep-sea-fan channel sequences (Winn and Dott, 1977).

The cobble and boulder lag on the stoss sides of the gravel waves may indicate that the upper surfaces of the gravel waves had been partially deflated by flow (as suggested by Baker, 1973, refering to boulder armour on the Giant Ripples of the Scablands). The mud drape is believed to represent deposition of a mud suspension generated as a result of the earthquake-induced failure and turbidity current. This mud settled out after the passage of the main body of the turbidity current. The variable thickness of the drape over the gravel waves may indicate that bedform morphology controlled the deposition of the mud drape. In the presence of weak downvalley flow (the 'tail' of the turbidity current) preferential deposition would occur in the lee of the wave crests. The increasing thickness of a normally graded drape down Eastern Valley may indicate that there was a progressive change from an erosional regime in the upper valley to a largely depositional regime in the lower valley. The thickening of the normally graded drape would serve to progressively bury the armoured

upper surface of the gravel waves which existed during the phase of active wave migration.

Ribbons and sand sheets

Valley-parallel streaks or ribbons have been described within the gravel wavefields of the middle valley (Piper et al., 1985, Fig. 6). These streaks become more common and widen downvalley. They can be up to 25km long, but rarely exceed 500m width. The ribbons bifurcate both up and down valley and in one example a series of thin closely spaced ribbons amalgamate into one large ribbon (Fig. 7).

The ribbons show up on SeaMARC images as regions of lower acoustic backscatter than the surrounding gravel wavefields. The ribbons are recognised on 12 kHz and 3.5 kHz profiles as a smooth, thin, high-amplitude surface reflector with no subbottom penetration (Fig. 8). This contrasts with the irregular overlapping-hyperbolic echo character associated with the gravel waves and the parallel, laterally-continuous sequence of subbottom reflectors characteristic of the levee muds. On airgun profiles the ribbons can be recognised as a smooth surface reflector over a thin transparent zone which overlies highly reflective sediment (Fig. 8). The ribbon surfaces appear smooth although their margins are locally seen to mimic adjacent gravel wave relief (Fig. 6b). South of the 3700m isobath, the ribbons expand laterally to become sheet deposits which are as extensive as the gravel wavefields. The surface of larger sheets show low relief which suggests that these sheets thinly drape underlying topography (Fig. 8).

A single core has been recovered in a 600m wide ribbon (Fig. 7). More than a metre of well sorted coarse sand was recovered which graded into mud in the top 40cm. A core taken in a valley floor channel (Fig. 9) in a region of similar acoustic backscatter failed to penetrate, recovering only traces of fine sand. The scratches on the core cutter implied that it had penetrated a sand deposit. Thus the contrasting intensity of acoustic backscatter seen on the valley floor is interpreted as a lithologic signature that can be used to distinguish the the cobble and boulder deposits associated with the gravel waves from the coarse sand of the streaks and ribbons.

The sand ribbons commonly delineate elongate bathymeytric lows, implying that these deposits are topographically restricted. The base of the valley floor channels are dominantly filled with sand. The wide sand sheets, however, located on the central valley floor do not appear to lie in bathymetric lows. One particular sand sheet, located on the middle valley floor (Fig. 8) appears to be elongate transverse to flow and may be related to local large-scale swells of the same orientation recognised from GLORIA images (Masson et al., 1985, Fig. 4).

On the basis of the evidence presented it is suggested that the ribbons and sheets are coarse sand deposits. These sand bodies overly the gravel waves and thus postdate the period of gravel wave formation. These sand deposits are finer grained and better sorted than the gravel wave sediments. Thus the sediment in the ribbons and sheets could have been derived by winnowing of the upper surfaces of the gravel waves (suggested by cobble and boulder armour on the gravel wave-tops). This would have taken place during the later part of turbidity current passage when the bed shear stress was no longer sufficently competent for gravel wave migration. The coarse sand, winnowed from the elevated gravel wave fields, preferentially resedimented in topographic depressions on the valley floor.

Erosional valley margins.

The valley margin is defined as the zone between the valley floor and undisturbed levee sediments. The valley margins north of $43^{o}30'N$ are narrow and steep. South of this the valley margins become wider and shallow.

It is apparent from SeaMARC images of the margins of lower Eastern Valley that the turbidity current in 1929 was not restricted to the valley floor. Using both SeaMARC images and 12 or 3.5kHz echo character the topographic distribution of flow-generated morphology on the valley margin can be determined. Five examples of flow generated morphology are identified from valley margins south of $43^{o}30'N$. These examples are used to constrain the upper limit of flow in the turbidity current.

1- On the east margin of the valley at 43^{o} 20'N gravel waves give way up the valley flank to

a region of low acoustic backscatter (mud) (Fig. 9). The bedforms are flow generated and their orientation suggest downvalley flow. In contrast a series of low mud ridges aligned along the valley wall strike suggest shallow gravity driven creep into the valley. The boundary between the two morphogenic terrains occurs 210 to 230m above the base of the marginal valley floor channel.

2- Flow parallel lineations on top of the northern section of the Interbranch High (SeaMARC 1984 JD 283/2300) suggest that this high was overwhelmed by flow. The maximum elevation of the high above the South and East Branch floors at this point is 110m.

3- Flow parallel lineations also occurs on the inside (west) wall of a bend in the South Branch (Fig. 10). Holocene sediment is absent in a piston core taken within the lineated terrain (Stow, 1981, Fig. 8, core #15). Red Pleistocene silty clay outcrops at the surface. by comparison with other cores in the levee, at least one metre of sediment has been stripped off the valley flank at this site. Lineated morphology is visible on sidescan up to 220m above the floor of South Branch.

4- Stripes of higher acoustic backscatter, seen on SeaMARC images, occur on the west side of the Interbranch High (Fig. 11). The orientation of the stripes suggests that although the South Branch thalweg meanders tightly, the flow was sufficently thick to flow directly over the flanks of the Interbranch High. Stripes are recognised 270m above the South Branch floor. The Holocene sediment from cores close to the axial crest of the Interbranch High are undisturbed (Stow, 1981, Fig. 8, core #36).Thus the crest of the high, which is elevated 300m above the South Branch floor, was not completely overwhelmed by flow.

5- The orientation of lineations and dunes on the north margin of the lower South Branch thalweg (Fig. 14a) suggests that there was flow from the East Branch across the southern end of the Interbranch High. Thus on the Valley Termination Zone, the flows from the two lower valley branches were no longer separate.

The steeper valley margins north of $43^{\circ}30'N$ are extensively incised by dendritic drainage gullies normal to the valley axis (the ridge and spur terrain of Piper et al., (1984, Fig. 5)). No overprinting of this gullied terrain by erosive morphology, indicative

of high energy downvalley flow, can be distinguished. Thus constraints on flow thickness, on the basis of SeaMARC images, cannot be imposed for the turbidity current north of 43°30'N.

On the basis of the evidence presented, the maximum elevation of the turbidity current can be constrained to have been about 220m in the middle valley, increasing to about 280m in the lower valley. In the lower valley, the turbidity current was divided on either of the Interbranch High. The two currents merged again in the Valley Termination Zone.

Macrodunes

Long wavelength (300m), periodic undulations, oriented transverse to inferred flow, occur in the Valley Termination Zone (Fig. 12 and 13a). On SeaMARC images, these features (termed macrodunes) are developed in a region of acoustic backscatter similar to the sand sheets and are thus probably coarse sand deposits. The macrodunes are symmetric bedforms, similar in morphology to antidunes.

Gravel wavefields and sand sheets coexist with (Fig 14b), and are replaced by, macrodune fields in the lower South Branch. In this region the valley relief diminishes to the SE. A shallow depression extends from the lower South Branch across the Valley Termination Zone. The thalweg of the depression lies between a low levee to the southwest of about 15m elevation and the downstream limit of the Interbranch High to the northeast.

The macrodunes are straight crested near the thalweg where they occur in lanes (Fig. 14a), but become sinuous both distally and on the adjacent levee to the south. The macrodunes are oriented in a radial pattern, the crests striking NNE-SSW in the thalweg, rotating clockwise to the south onto the low southern levee. The amplitude of the macrodunes must be less than about 4m, as the relief due to these bedforms cannot be directly observed from subbottom bathymetry and can only be resolved on the outer part of SeaMARC images (at low grazing angles).

On the crest of the low levee, lineations are developed parallel to the inferred flow direction. Small scale transverse bedforms, similar to gravel waves, are developed along the length of some lineations (fig. 12). These lineations overprint and thus postdate the

macrodunes. Within the lineated region, 3m of granule to pebble gravel was cored which grades to mud in the top 50cm. Downstream of these lineations, a series of ragged crest with the same orientation as the macrodune crest occur (Fig. 13b). These may indicate that the levee top sediment has been eroded.

Long wavelength (450-600m) swells resembling macrodunes occur in middle Eastern Valley and in East Branch. Gravel waves are superimposed on these swells (Fig. 13a). These swells are best developed on the central valley floor adjacent to the marginal valley floor channels.

In the lower reaches of the South and East Branches, the levees, which were capable of laterally constraining turbidity current flow (270 to 300m thick), diminish rapidly. In the Valley Termination Zone, however, turbidity currents are free to expand laterally. The observed radial orientation of macrodune crests could have been generated by such laterally expanding flow.

DISCUSSION

Morphology

The morphology of Eastern Valley is unlike that of most other large fan valleys. The wide floor, high levees and anomalously coarse sediment suggest a unique sediment supply and transport relationship. The channels entrenched within the valley floor do not make up a continuous thalweg and thus are not zones within the floor in which low volume turbidity current flow have been confined. Rather the location of the channels may indicate zones of locally enhanced bed shear stress (and thus erosion) adjacent to lateral boundaries. Such enhanced bed shear stress could result from increased secondary flow generated as a result of horizontal velocity shear in large volume flow due to friction against the adjacent margin. An alternate explanation of the channel locations may be that erosion preferentially takes place into the soft levee sediments, rather than into the much coarser valley floor deposits. Such a mechanism would result in lateral expansion, rather than entrenchment of the valley floor. The anomalously wide floor could have been developed in

this manner. The morphology of the valley floor would thus be a direct result of the extremely coarse sediment in the valley, derived by erosion of Pleistocene proximal glaciomarine sediments on the upper slope.

Bedforms

The presence of bedforms on the valley floor implies that recent traction flow has taken place. These surficial bedforms must have been generated by the 1929 turbidity current, as the velocities indicated from cable break data exceed the bedload transport thresholds of the coarse valley floor sediments in which the bedforms are developed. The superposition of sand sheets and ribbons on the gravel waves indicate that the bedforms were generated in a flow regime of waning competence. At the same time the valley margins were eroded by the turbidity current which was several hundred metres thick. Mud, eroded from the valley margins, was incorporated into the lower valley floor sediments. In the valley termination zone the turbidity current was able to laterally spread across the proximal fan lobe. Macrodunes were generated during this phase of flow.

Turbidity current evolution

Sediment failure in the watershed region of Eastern Valley resulted in a turbidity current. This turbidity current generated bedforms along the valley floor and on the proximal fan lobe. Some bedforms occur on the upper valley, indicating that turbidity current flow was initiated close to the epicentre. The region of known sediment failure, however, included the upper and half of the middle of Eastern Valley (the extent of instantaneous cable breaks). Thus additional suspended sediment, generated by earthquake-triggered failure, was available to contribute to the turbidity current along this stretch of valley.

The turbidity current in Eastern Valley merged with a turbidity current from Grand Banks Valley. The combined flow, was divided on either side of the Interbranch High. The resulting two turbidity currents remerged in the Valley Termination Zone at which point the combined

flow was free to laterally spread across the proximal depositional lobe of the Laurentian Fan.

Acknowledgements.

Financial support for the work was provided by the Office of Naval Research grant to Dalhousie University (N00014-83-G-0114) and a Killam Memorial Scholarship. I thank the officers and crew of C.S.S. Hudson and M.V. Pandora II. The report was reviewed by David Piper and Larry Mayer.

REFERENCES

Baker,V.R.,1973, Paleohydrology and sedimentology of Lake Missoula flooding in Eastern Washington: The Geological Society of America, Special paper 144.

Bretz,J.H.,Smith,H.T.U. and Neff,G.E.,1956, Channeled Scablands of Washington: new data and interpretations: The Geological Society of America Bulletin, v.67, p.957-1049.

Doxsee,W.W.,1948, The Grand Banks Earthquake of November 18, 1929: Publications of the Dominion Observatory Ottawa, v.7, no.7, p.323-335.

Emery,K.O.,Uchupi,E.,Phillips,J.D.,Bowin,C.O.,Bunce,E.T. and Knott,S.T.,1970, Continental rise off eastern North America: American Association of Petroleum Geologists Bulletin, v.54, p.44-108.

Fruth,L.S.,1965, The 1929 Grand Banks turbidite and the sediments of the Sohm abyssal plain: M.Sc. thesis, Columbia University, New York, 258p.

Heezen,B.C.and Ewing,W.M.,1952, Turbidity currents and submarine slumps, and the 1929 Grand Banks earthquake: American Journal of Science, v.250, p.849-873.

Heezen,B.C.,Ericson,D.B. and Ewing,W.M.,1954, Further evidence for a turbidity current following the 1929 Grand Banks earthquake: Deep Sea Research, v.1, p.193-202.

Hughes Clarke,J.E.,Mayer,L.A.,Piper,D.J.W. and Shor,A.N.,1986, Pisces IV submersible dives in the epicentral region of the 1929 Grand Banks earthquake: Geological Survey of Canada Paper, in press.

Kindle,E.M.,1931, Sea bottom samples from the Cabot St. earthquake zone: The Geological Society of America Bulletin, v.42, p.557-574.

Kosalos,J.G. and Chayes,D.N.,1983, A portable system for ocean bottom imaging and charting: OCEANS 83 (Proceedings of the Third working Symposium on Oceanographic Data Systems), p.1-8.

Malde,H.E.,1968, The catastrophic Late Pleistocene Bonneville Flood in the Snake River Plain, Idaho: United States Geological Survey, Professional paper 596.

Malinverno,A.,Ryan,W.B.F.,Auffret,G.I. and Pautot,G.,1987, Sonar Images of the Path of Failure Events on the Continental Margin off Nice, France: Geological Society of

America, Special Paper. in press.

Masson,D.G.,Gardner,J.V.,Parson,L.M. and Field,M.E.1985, Morphology of Upper Laurentian Fan using GLORIA Long-range Side-scan sonar: American Association of Petroleum Geologists Bulletin, v.69 p.950-959.

Meagher,L.,1984, Interpretation of Quaternary and Upper Neogene seismic stratigraphy on the continental slope off St. Pierre Bank: Geological Survey of Canada, Open File no. 1077.

Menard,H.W.,1964, Marine Geology of the Pacific: McGraw-Hill Book Co., New York, NY, 271p.

Piper,D.J.W. and Normark,W.R.,1982, Acoustic interpretation of Quaternary sedimentation and erosion on the channelled upper Laurentian Fan, Atlantic margin of Canada: Canadian Journal of Earth Sciences, v.19, p.1974-1984.

Piper,D.J.W.,D.A.V.Stow and W.R.Normark,1984, The Laurentian Fan: Sohm Abyssal Plain: Geo-Marine Letters, v.3, p.141-146.

Piper, D.J. W., Sparkes, R., Mosher, D.C., Shor, A.N. and Farre, J.A., 1984, Seabed instability near the epicentre of the 1929 Grand Banks Earthquake: Geological Survey of Canada, Open file report no.1131.

Piper,D.J.W.,Shor,A.N.,Farre,J.A.,O'Connell,S. and Jacobi,R.,1985, Sediment slides and turbidity currents on the Laurentian Fan: Sidescan sonar investigations near the epicentre of the 1929 Grand Banks earthquake: Geology, v.13, p.538-541.

Piper,D.J.W. and Aksu,A.E.,1987, The source and origin of the 1929 Grand Banks turbidity current inferred from sediment budgets: in review for Geo-Marine Letters.

Piper,D.J.W.,Shor,A.N. and Hughes-Clarke,J.E.,1987, The 1929 Grand Banks earthquake, slump and turbidity current: Geological Society of America, Special Paper, in press.

Sanders,J.E.,1969, Sediments of three box cores from axis of submarine canyon west of Grand Banks, off Newfoundland (abstract): Geological Association of Canada and Mineralogical Association of Canada, Joint Annual Meeting, Montreal, 5-7 June 1969, p.44-45.

Stow,D.A.V.,1977, Late Quaternary stratigraphy and sedimentation on the Nova Scotian outer

continental margin: Unpublished doctoral dissertation, Dalhousie University, 360p.

Stow,D.A.V.,1981, Laurentian Fan: morphology, sediments, processes, and growth pattern: American Association of Petroleum Geologists Bulletin, v.65 p.375-393.

Wilson,E. and Piper,D.J.W.,1985, Seismic stratigraphy of the Laurentian fan: Geological Survey of Canada, Open file report no.1231.

Winn,R.D.Jr. and Dott,R.H.Jr.,1977, Large scale traction-produced structures in deep-water fan-channel conglomerates in southern Chile: Geology, v.5, p.41-44.

FIGURES

Figure 1: Diagram showing the relationship of deep-sea cables and cable breaks to the drainage of the Upper and Middle Laurentian Fan. Channel pattern north of 42° 40'N based on GLORIA survey of Masson et al. 1985, to the south based on bathymetry and echo character data from B.I.O. cruises.

Figure 2: Bathymetry of the Laurentian Fan, north of 41°N. Compilation based on C.H.S. charts 801, 802 and Nk-21-B. Fourfold physiographic zonation of Eastern Valley is superimposed. (U.) Upper valley, (M.) Middle valley, (L.) Lower valley, (V.T.Z.) Valley Termination Zone.

Figure 3: Location of all SeaMARC lines run on the Laurentian Fan. Location of Mosaic Sheets (Plates I-XI) and SeaMARC images (Figures 6 to 14).

Figure 4: Position of all bottom samples and camera stations on the Upper and Middle Laurentian Fan. Inset shows location of Figure 5, showing detail of area around epicentre of 1929 Grand Banks earthquake.

Figure 5: Position of all bottom samples and camera stations around the epicentre of the 1929 Grand Banks earthquake. Morphogenic zones based on SeaMARC interpretation of Piper et al. (1985, Fig. 1).

Figure 6: (a) SeaMARC 5km swath image of gravel wave field with sand ribbons.
(b) SeaMARC 5km swath image of ellipsoidal regions of gravel waves within a major sand sheet.

Figure 7: SeaMARC 5km swath image of wide sand ribbon in gravel wave field. Interpretation diagram of image, showing position of cores 85-001 7, 8, 9.

Figure 8: Composite diagram with 5km SeaMARC sidescan, synchronous 4.5 kHz subbottom profile, surface 3.5 kHz record and 40 cu. in. airgun record of wide sand sheet on the floor of Eastern Valley.

Figure 9: Composite diagram including 2km swath SeaMARC sidescan across the east marginal valley floor channel, 4.5 kHz subbottom profile and interpretation diagram showing position of core 85-001 10 and camera station #2 of 85-001.

Figure 10: Composite diagram including 2km swath SeaMARC sidescan across South Branch floor and western valley margin, 4.5 kHz subbottom profile and interpretation diagram showing position of camera station #4 of 85-001.

Figure 11: Composite diagram including 5km swath SeaMARC sidescan acoss Interbranch High and South Branch, 4.5kHz subbottom profile and interpretation diagram showing bathymetry and the position of cores 84-040 1, 2, 3.

Figure 12: Composite diagram including 2km swath SeaMARC sidescan acoss macrodunes and lineations and interpretation diagram showing position of core 85-001 15 and camera station #3 of 85-001.

Figure 13:(a) SeaMARC 5km swath image of trough and swells on Eastern Valley floor with gravel waves and sand streaks superimposed.

(b) SeaMARC 5km swath image from Valley Termination Zone, showing macrodunes and ragged crests.

Figure 14:(a) SeaMARC 5km swath image across laned macrodunes in southern limit of South Branch thalweg and obliquely oriented bedforms on slightly elevated zone to the north.

(b) SeaMARC 2km swath image in South Branch thalweg, showing coexistance of gravel waves and macrodunes.

Plates I to XI: Mosaic of SeaMARC I imagery along Eastern Valley. For location of Mosaic segments, see Figure 3. Scale approximately 1 : 200,000.

Table : 1

Laurentian Fan Cores.

cruise	#	depth (m)	latitude	longitude	
VMØ2	1	2184	44 18	56 19	
	2	2878	44 15	56 Ø	
	3	42Ø4	43 15	55 45	
	4	4Ø76	43 15	56 17	
	5	33Ø7	43 5Ø	54 44	
	6	4314	43 12	54 16	just TWC
	7	466Ø	42 47	54 47	
	8	4217	42 43	55 55	
	9	47Ø2	42 28	54 54	
	1Ø	4846	41 51	53 7	washed out
	11	4874	41 42	53 16	washed out
VM17	178		43 23	54 52	
VM27	7a	5Ø74	41 27.5Ø	52 37.8Ø	washed out
	7	4612	42 47.4Ø	54 2Ø.4Ø	
	8	5152	4Ø 48.1Ø	56 36.ØØ	
	12		44 17.ØØ	55 39.ØØ	
?	1	4Ø31	43 31.5	55 16.Ø	box core
Sanders,	2	4Ø31	43 3Ø.Ø	55 12.Ø	box core
1969	3	4144	43 11.5	55 6.5	box core
H73-Ø11	6	4649	42 39.6Ø	54 3.4Ø	
	7	4642	42 18.8Ø	54 27.8Ø	
	8	471Ø	42 1Ø.4Ø	54 36.3Ø	
	9	4574	41 59.4Ø	54 48.1Ø	
	1Ø	4574	41 59.4Ø	54 48.1Ø	
H73-Ø31	7	4Ø55	42 58.7Ø	55 14.9Ø	
	8	4562	42 32.5Ø	55 22.2Ø	
	9	428Ø	42 18.1Ø	56 1.ØØ	
	1Ø	4334	42 22.1Ø	56 22.6Ø	
	11	4355	42 21.5Ø	56 25.5Ø	
H74-Ø21	9	4389	42 26.ØØ	55 47.8Ø	
	1Ø	437Ø	42 27.8Ø	55 46.8Ø	
	11	4346	42 28.ØØ	55 44.5Ø	
	12	45ØØ	42 35.ØØ	54 58.4Ø	
	13	456Ø	42 33.5Ø	54 52.ØØ	
	14	4489	42 32.4Ø	54 46.1Ø	
	15	4477	42 33.2Ø	54 49.3Ø	
	31	464Ø	42 27.7Ø	53 55.9Ø	
	32	4615	42 22.8Ø	54 32.4Ø	
	33	4454	42 2Ø.9Ø	54 4Ø.7Ø	
	34	4429	42 2Ø.3Ø	54 44.3Ø	
	35	449Ø	42 18.3Ø	54 51.2Ø	
	36	4194	42 6.2Ø	55 51.2Ø	

Table : 1

Laurentian Fan Cores.

cruise	#	depth (m)	latitude	longitude	
	37	4136	42 6.ØØ	55 53.ØØ	
D81-Ø44	7	2955	44 5.27	55 53.86	washed out
	8	3112	44 6.34	55 54.68	washed out
	9	2614	44 4.67	56 Ø.Ø8	gravity
	1Ø	273Ø	43 3Ø.77	55 49.63	gravity
	11	2786	43 32.14	55 49.47	gravity
D84-ØØ3	2		44 33.35	56 8.77	
	3	2Ø13	44 31.49	56 3.59	
H84-Ø4Ø	1	4579	42 21.19	55 4.13	
	2	4669	42 18.41	55 1.19	
	3	4613	42 19.54	55 Ø.81	
H85-ØØ1	7	311Ø	44 6.41	55 46.69	
	8	3Ø8Ø	44 7.42	55 45.63	
	9	3162	44 4.47	55 46.29	
	1Ø	4345	43 8.76	55 24.43	
	15	4873	41 31.Ø4	53 25.98	
	C2	4215	43 8.5Ø	55 25.5Ø	camera
	C3	485Ø	41 32.1Ø	53 27.1Ø	camera
	C4	452Ø	42 39.4Ø	55 2Ø.5Ø	camera
PN85-Ø59	1		44 42.48	56 6.56	shipek
	2		44 38.45	56 1Ø.8Ø	shipek
	3		44 35.36	56 1Ø.58	shipek
	C2		44 38.76	56 1Ø.95	camera
	C3		44 3Ø.37	56 4.15	camera
	C4		44 44.54	56 5.23	camera
	C5		44 38.35	56 7.47	camera
	C6		44 34.52	55 51.29	camera
	164Ø		44 32.6Ø	56 8.35	Pisces IV
	1641		44 43.8Ø	56 9.6Ø	Pisces IV
	1642		44 42.74	55 55.81	Pisces IV
	1643		44 36.36	55 47.1Ø	Pisces IV

Figure 1:

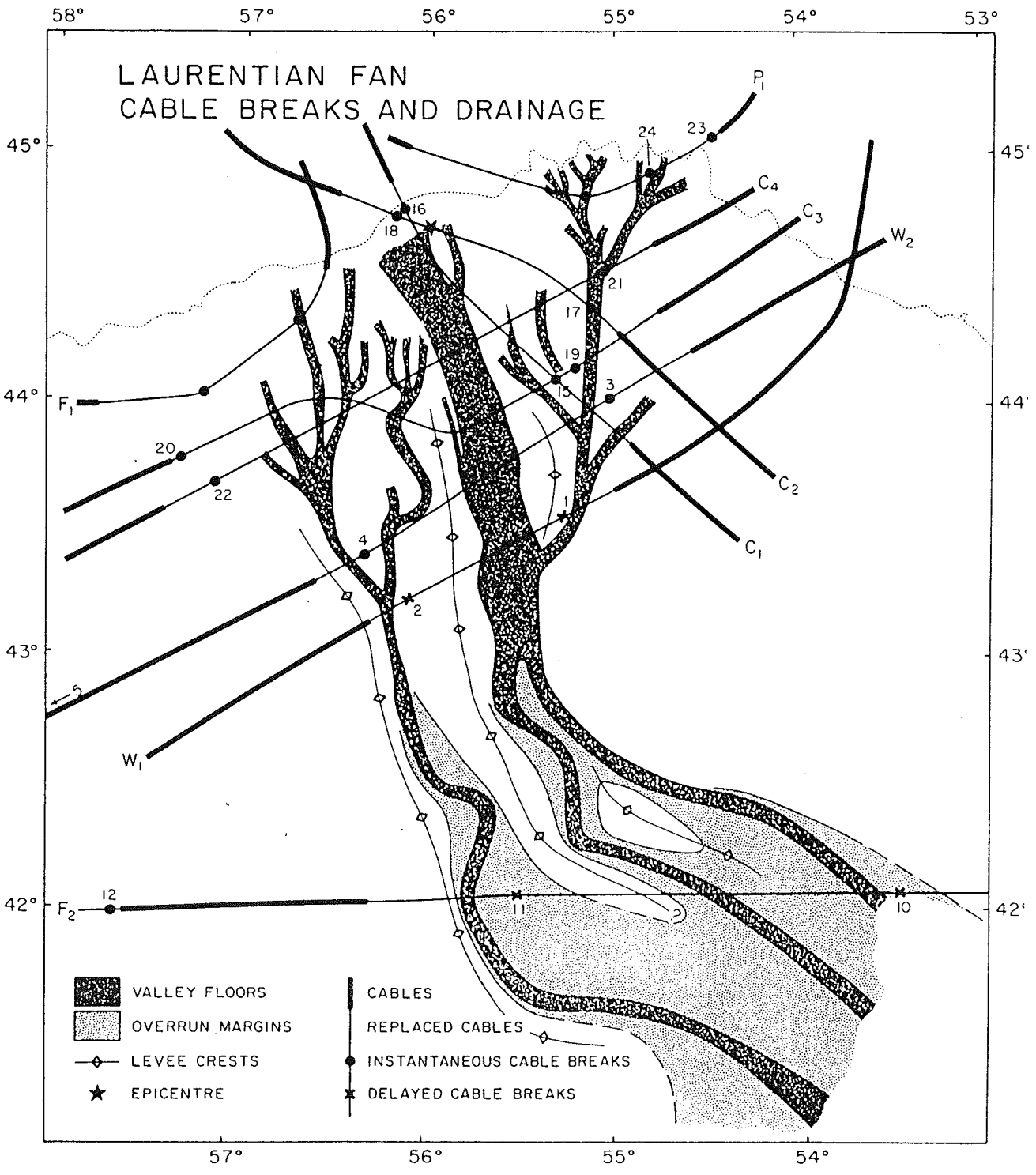
LAURENTIAN FAN
CABLE BREAKS AND DRAINAGE
58°
57°
56°
55°
54°
53°
45°
44°
43°
42°
45'
44'
43'
42'
P1
C4
C3
W2
C2
C1
F1
W1
F2
16
18
24
23
21
17
19
15
3
20
22
1
4
2
5
12
11
10
VALLEY FLOORS
OVERRUN MARGINS
LEVEE CRESTS
EPICENTRE
CABLES
REPLACED CABLES
INSTANTANEOUS CABLE BREAKS
DELAYED CABLE BREAKS

Figure 2:

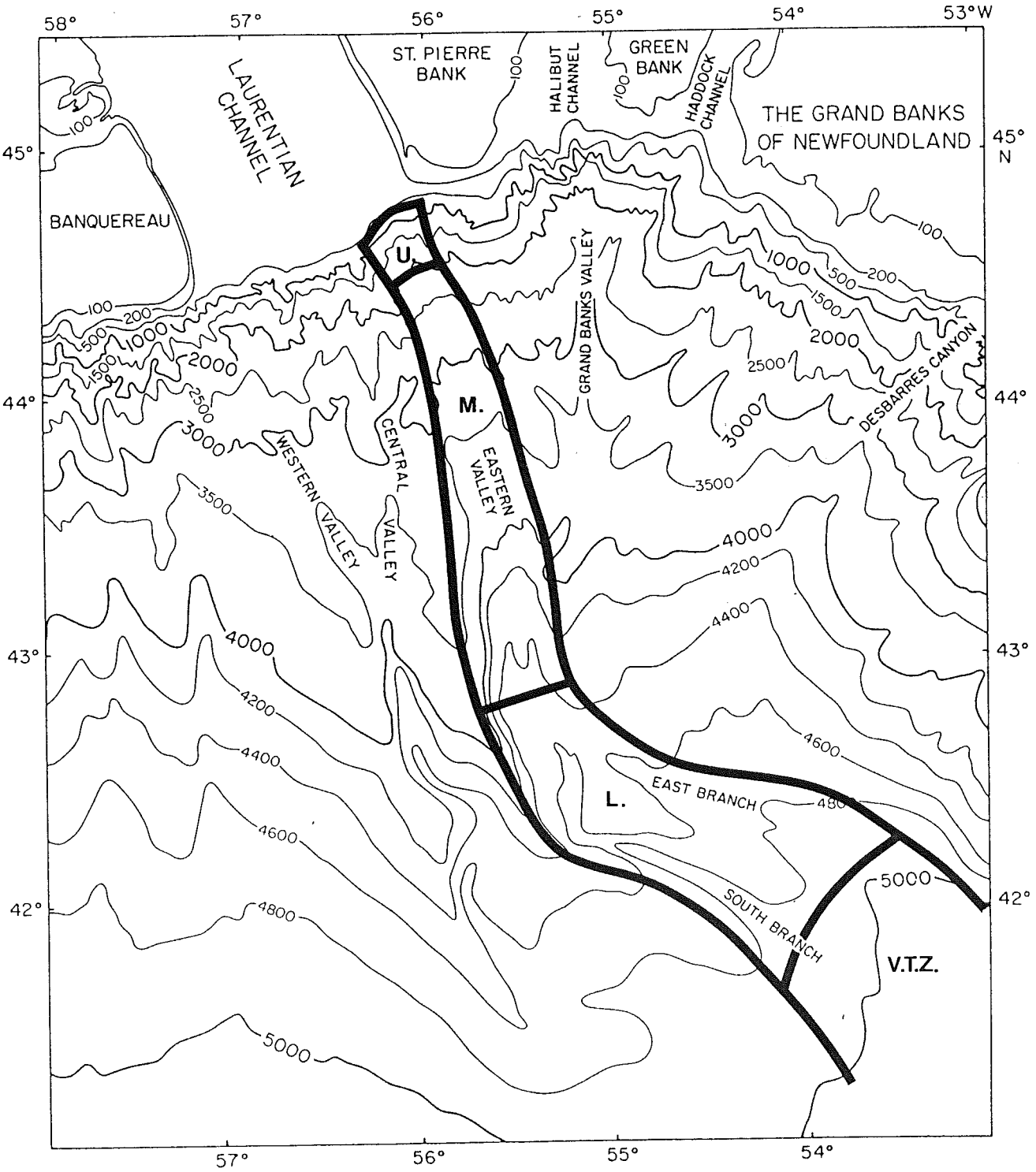
58°
57°
56°
55°
54°
53°W
45°
45° N
44°
43°
42°
ST. PIERRE BANK
LAURENTIAN CHANNEL
HALIBUT CHANNEL
GREEN BANK
HADDOCK CHANNEL
THE GRAND BANKS OF NEWFOUNDLAND
BANQUEREAU
U.
M.
L.
GRAND BANKS VALLEY
DESBARRES CANYON
WESTERN VALLEY
CENTRAL VALLEY
EASTERN VALLEY
EAST BRANCH
SOUTH BRANCH
V.T.Z.
100
200
500
1000
1500
2000
2500
3000
3500
4000
4200
4400
4600
4800
5000

Figure 3:

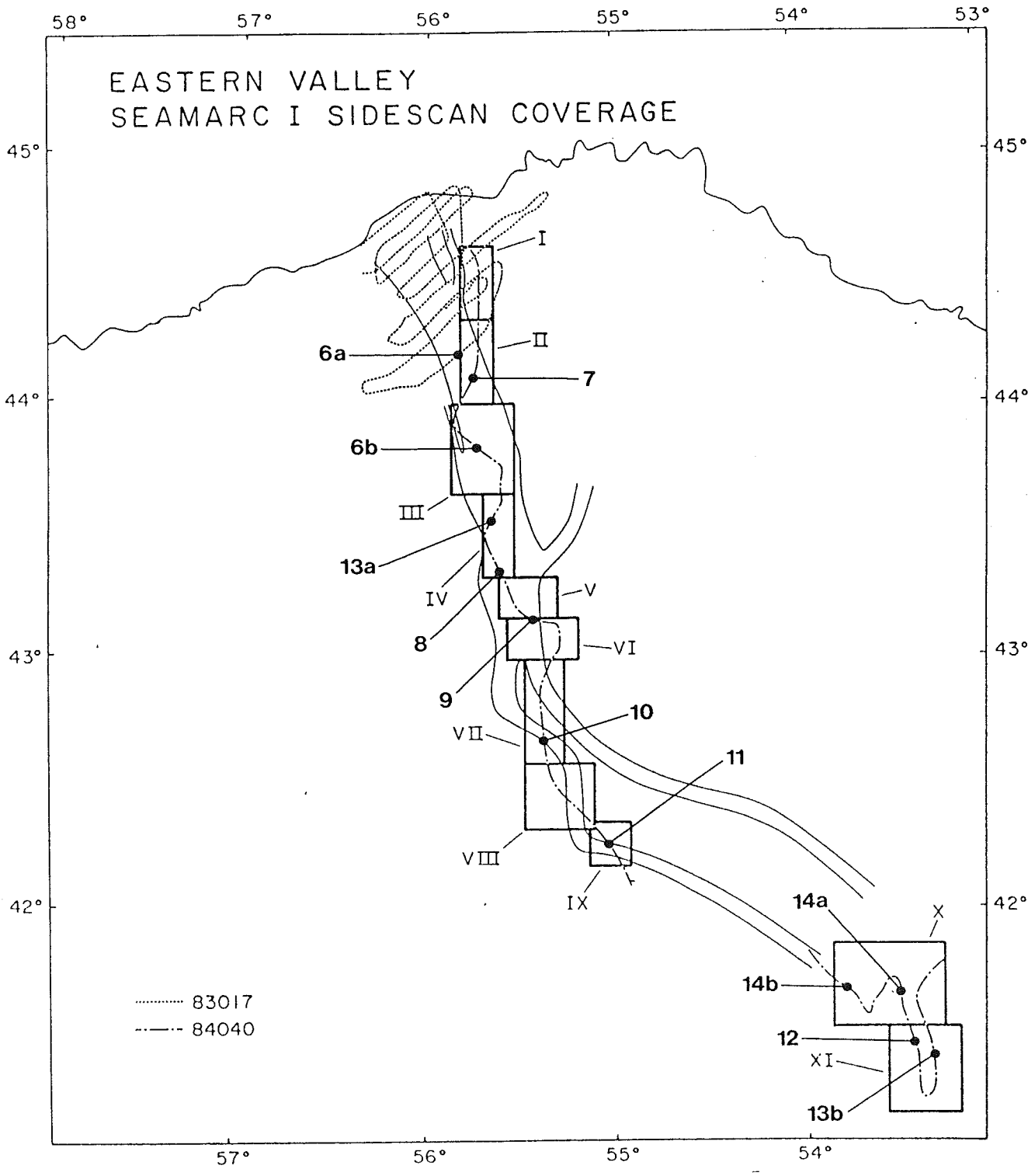
EASTERN VALLEY
SEAMARC I SIDESCAN COVERAGE
58°
57°
56°
55°
54°
53°
45°
44°
43°
42°
I
II
III
IV
V
VI
VII
VIII
IX
X
XI
6a
6b
7
8
9
10
11
12
13a
13b
14a
14b
83017
84040

Figure 4:

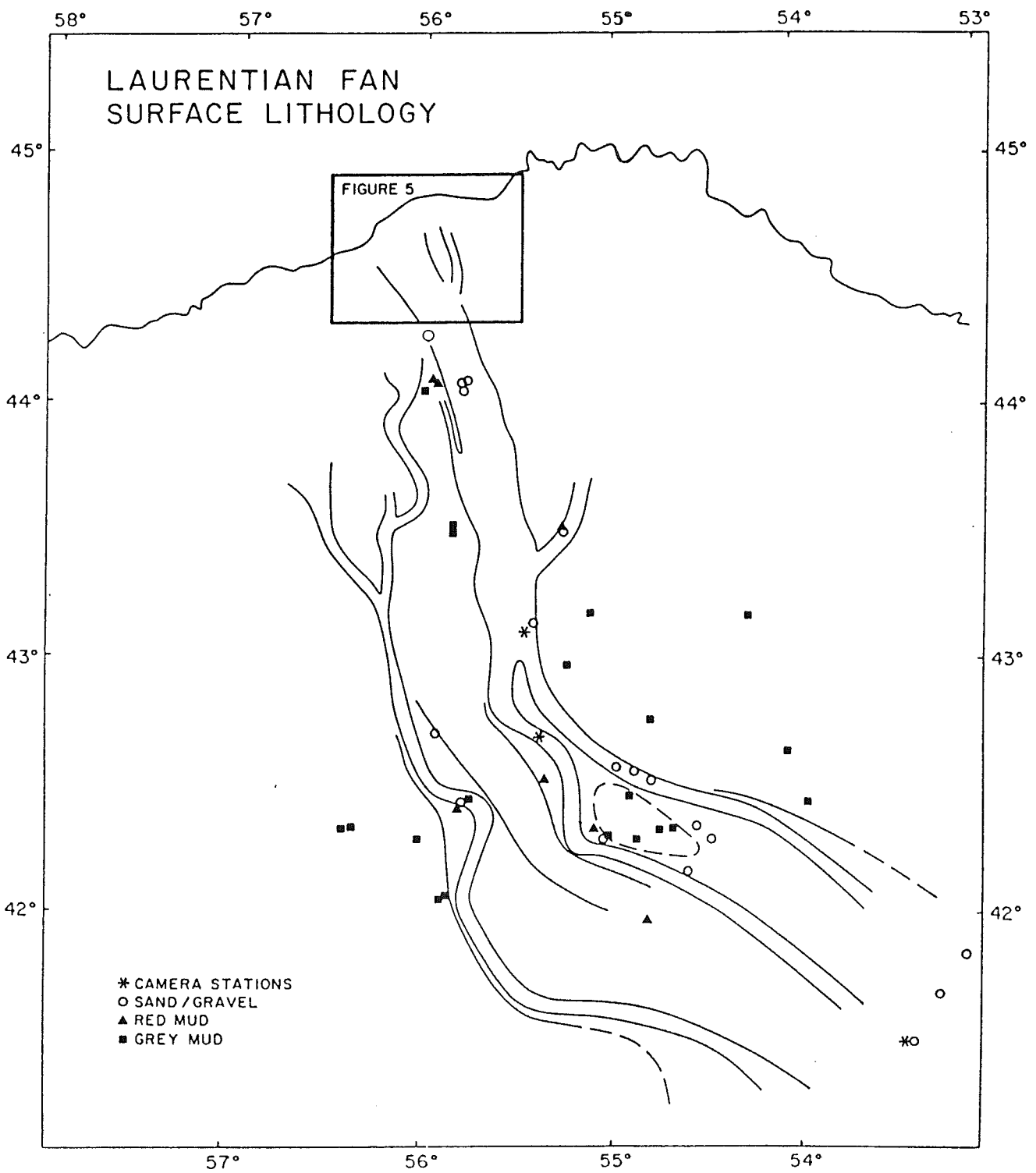
LAURENTIAN FAN
SURFACE LITHOLOGY
FIGURE 5
58°
57°
56°
55°
54°
53°
45°
44°
43°
42°
* CAMERA STATIONS
O SAND / GRAVEL
▲ RED MUD
■ GREY MUD

Figure 5:

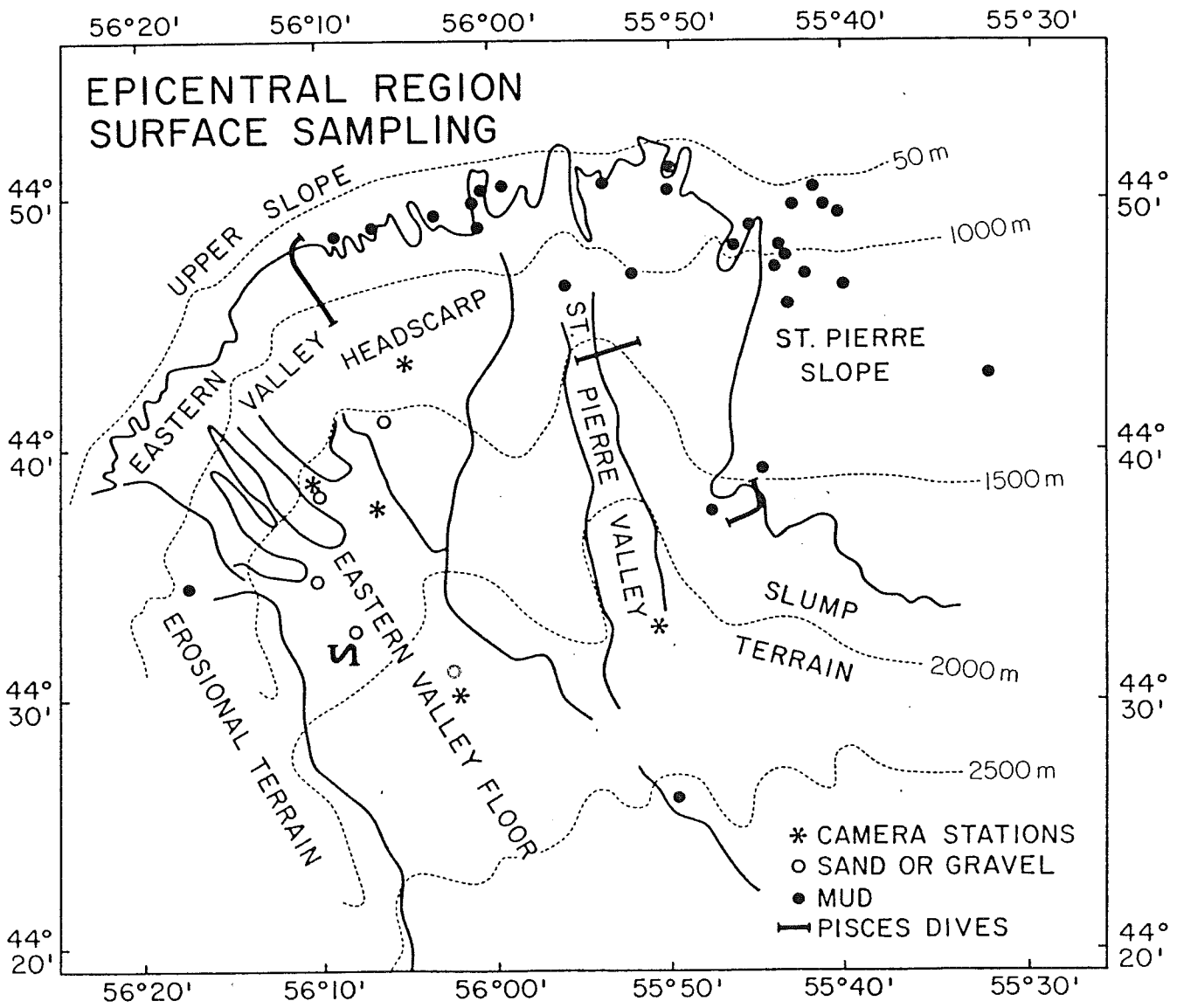
EPICENTRAL REGION
SURFACE SAMPLING
56°20'
56°10'
56°00'
55°50'
55°40'
55°30'
44° 50'
44° 40'
44° 30'
44° 20'
50 m
1000 m
1500 m
2000 m
2500 m
UPPER SLOPE
EASTERN VALLEY
HEADSCARP
ST. PIERRE VALLEY
ST. PIERRE SLOPE
SLUMP TERRAIN
EASTERN VALLEY FLOOR
EROSIONAL TERRAIN
* CAMERA STATIONS
o SAND OR GRAVEL
• MUD
PISCES DIVES

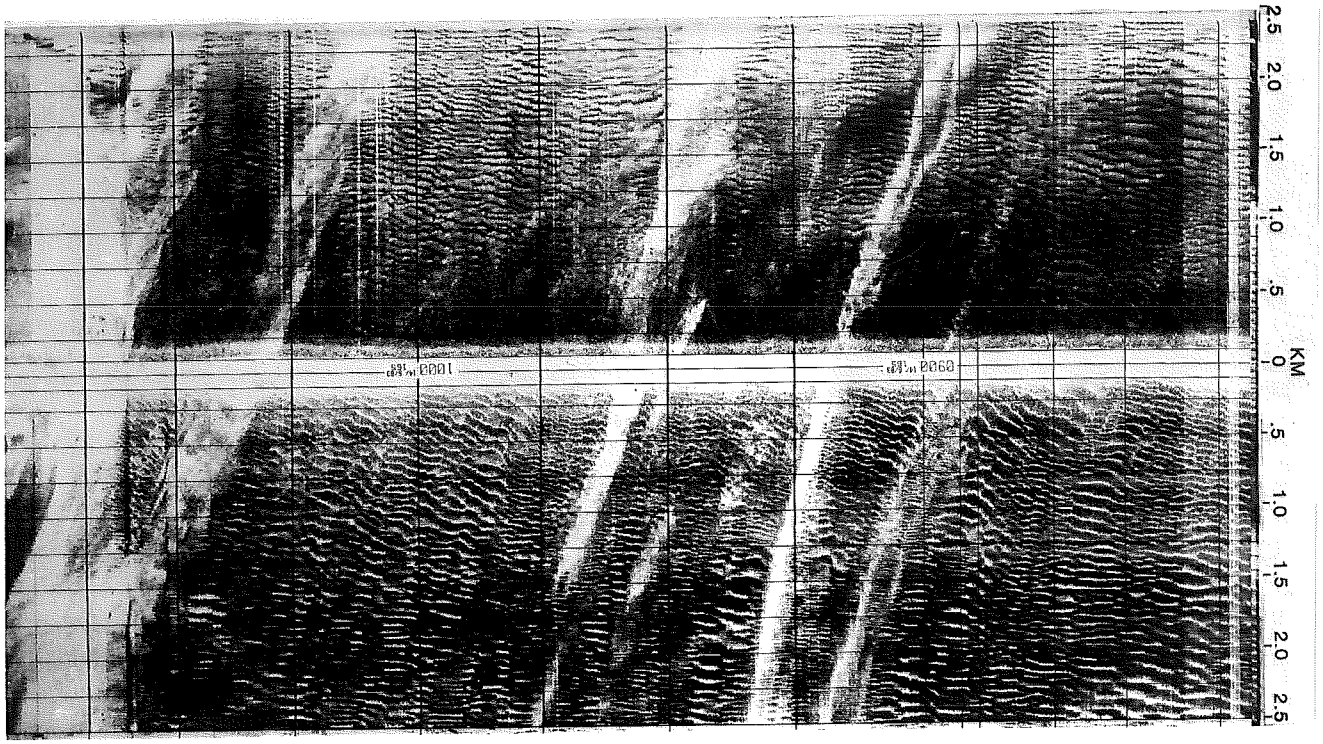

Figure 6a:

Figure 6b:

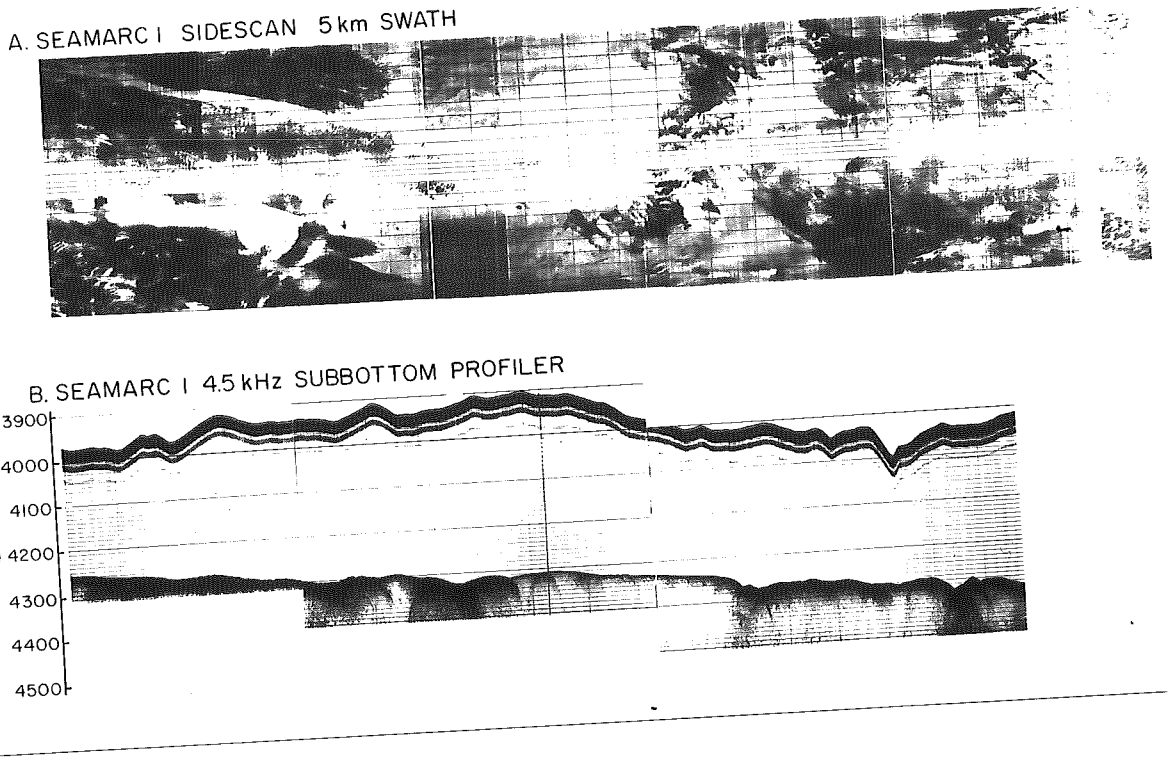

Hughes Clarke, 1987.

Figure 8:

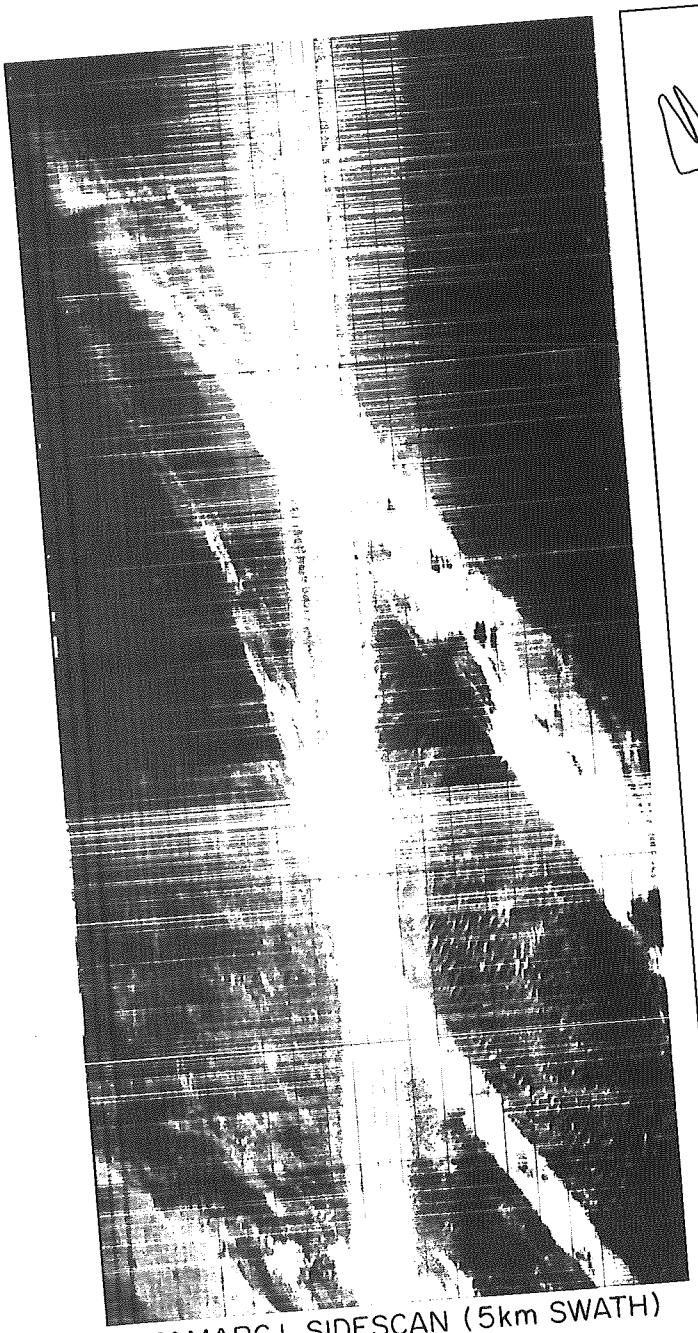

SEAMARC I SIDESCAN (5km SWATH)

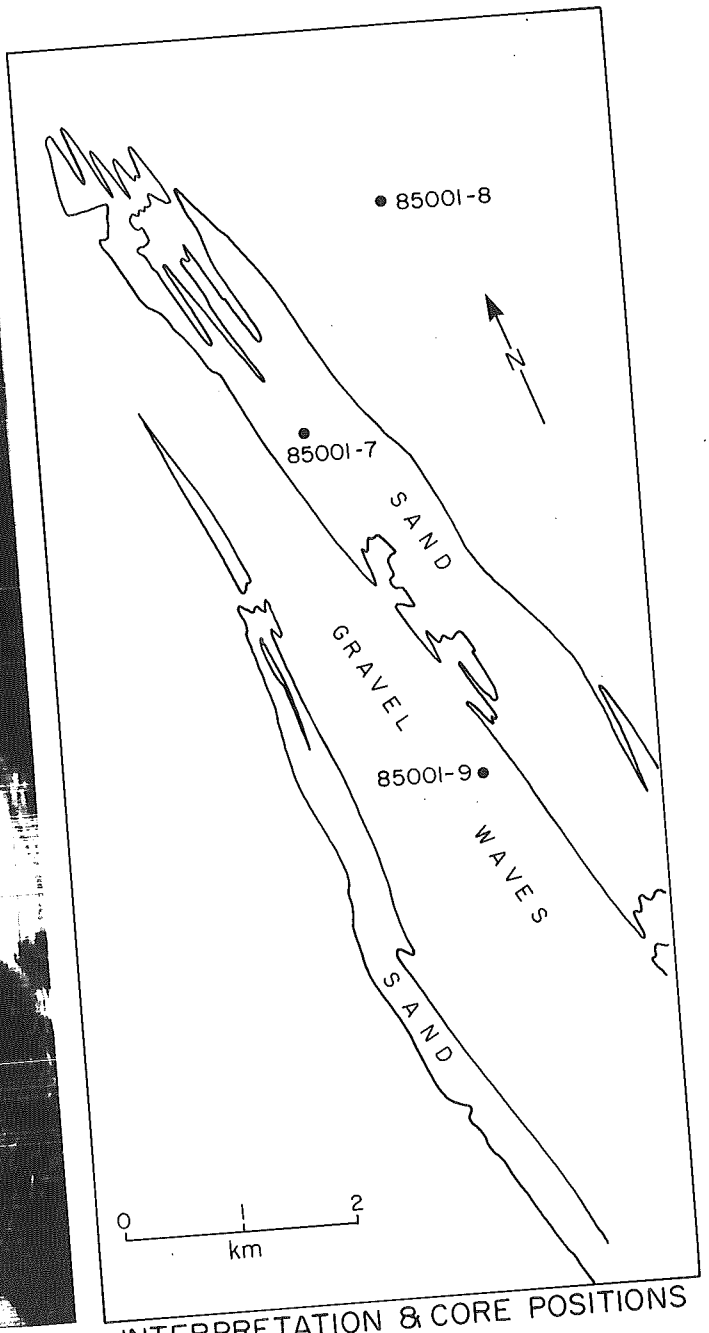

INTERPRETATION & CORE POSITIONS

Hughes Clarke, 1987.

Figure 7:

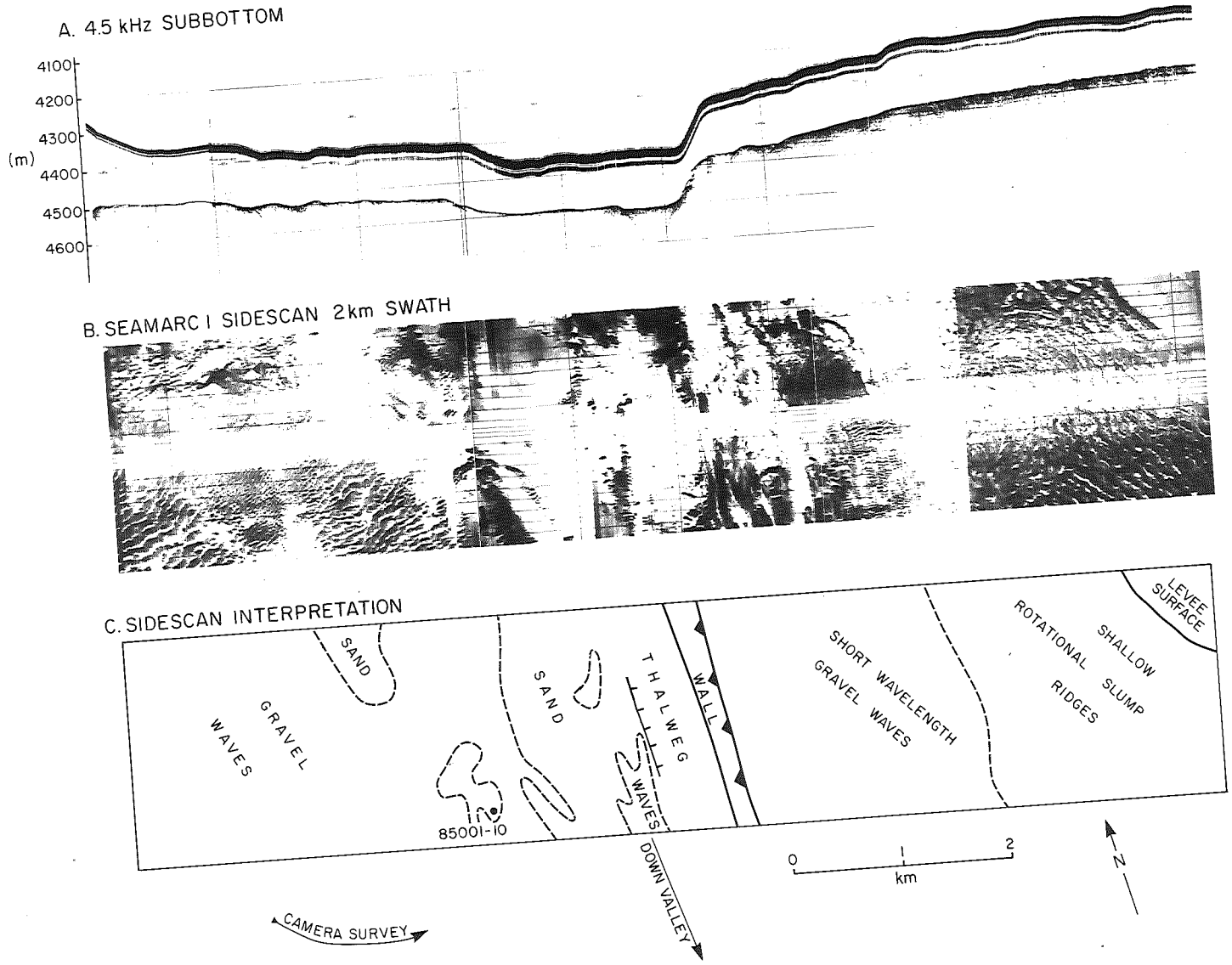

Hughes Clarke, 1987.

Figure 9:

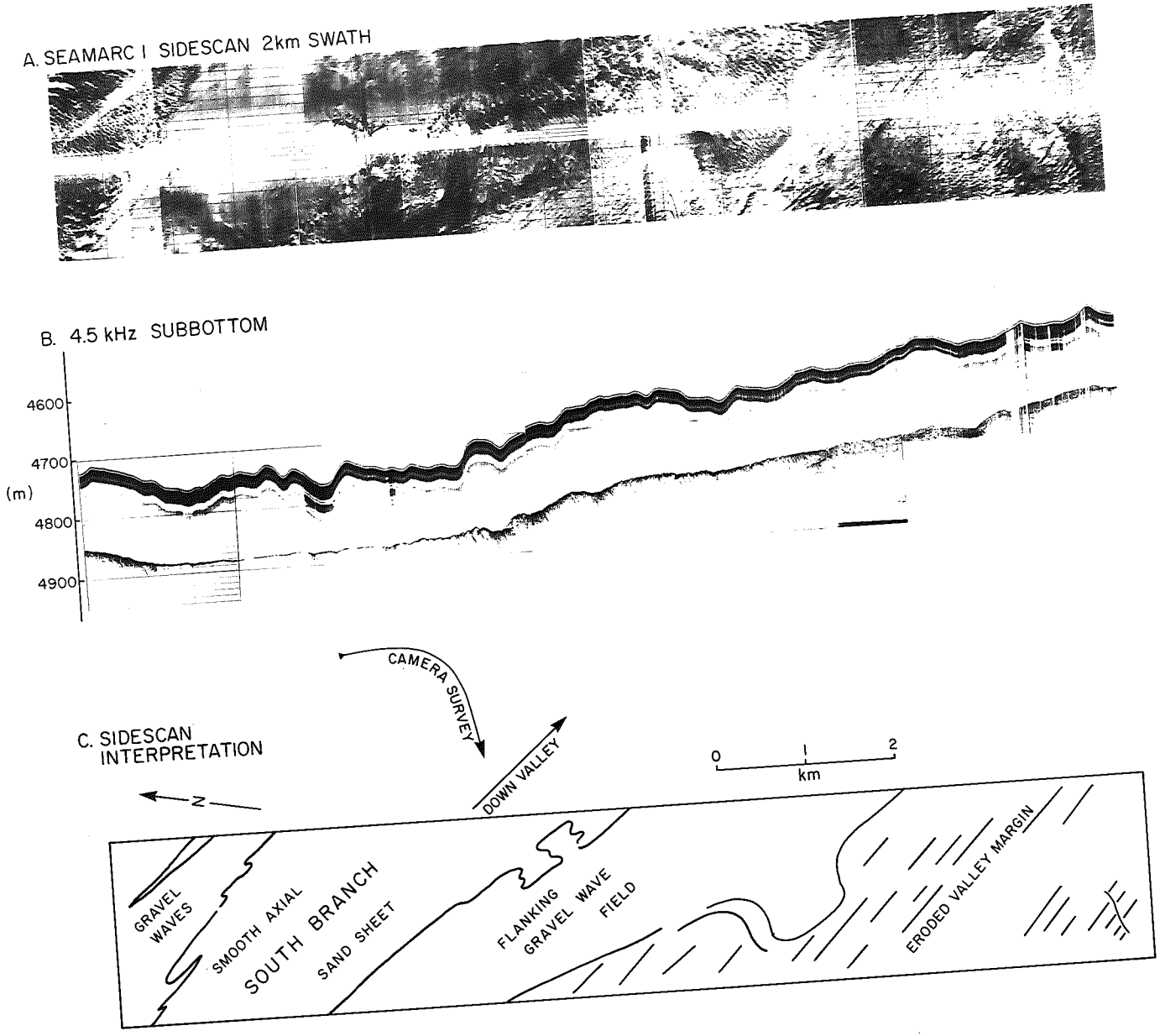

Hughes Clarke, 1987.

Figure 10:

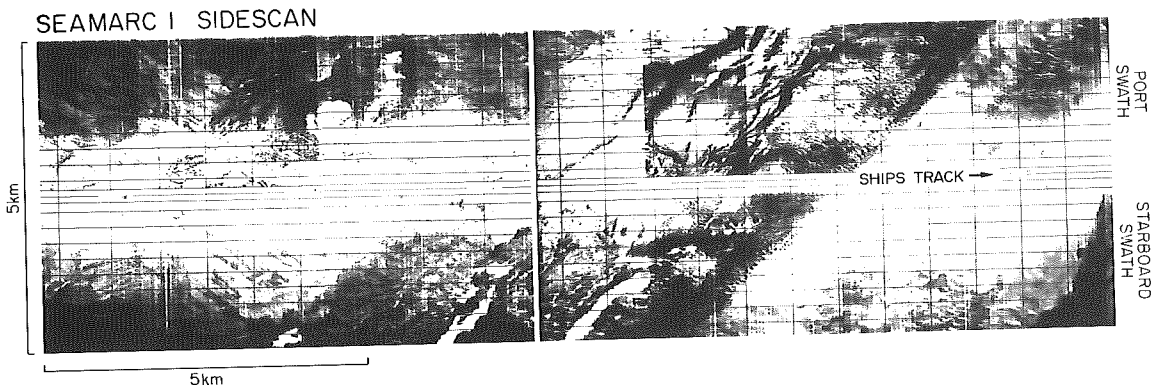

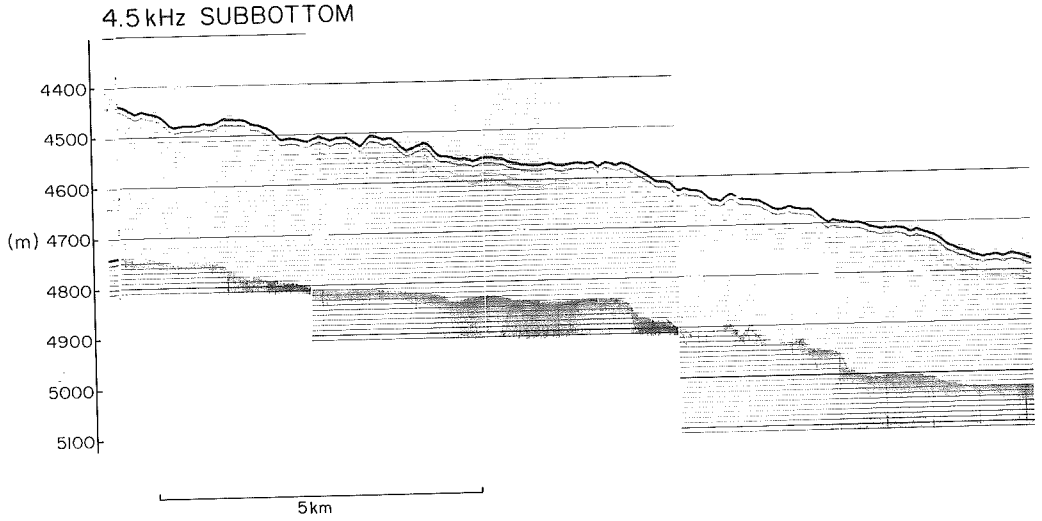

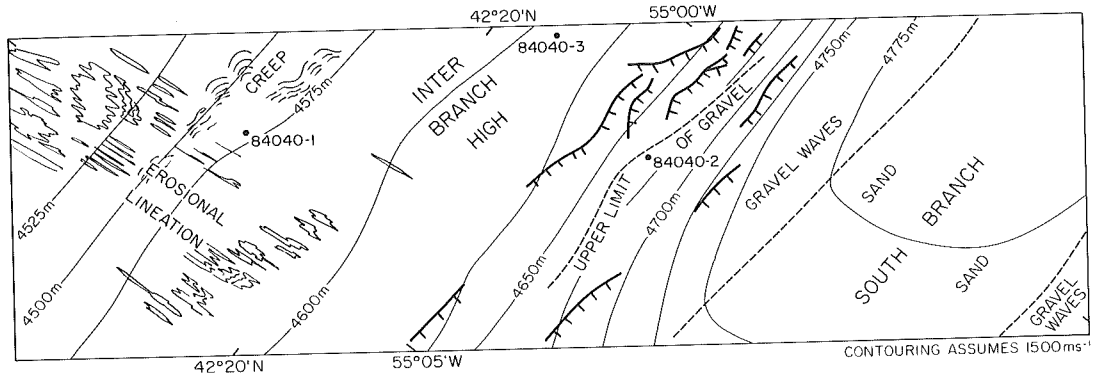

Hughes Clarke, 1987.

Figure 11:

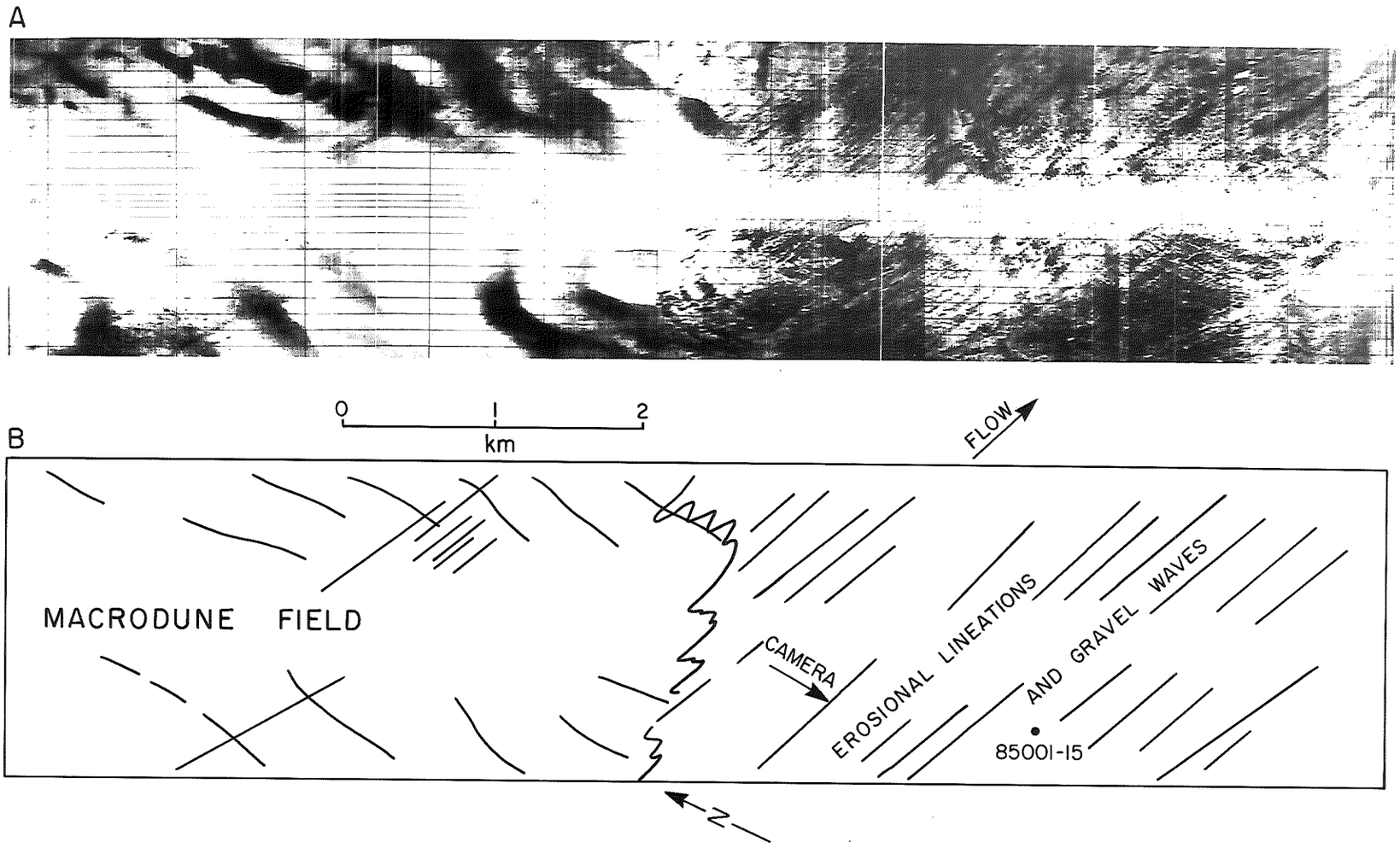

Hughes Clarke, 1987.

Figure 12:

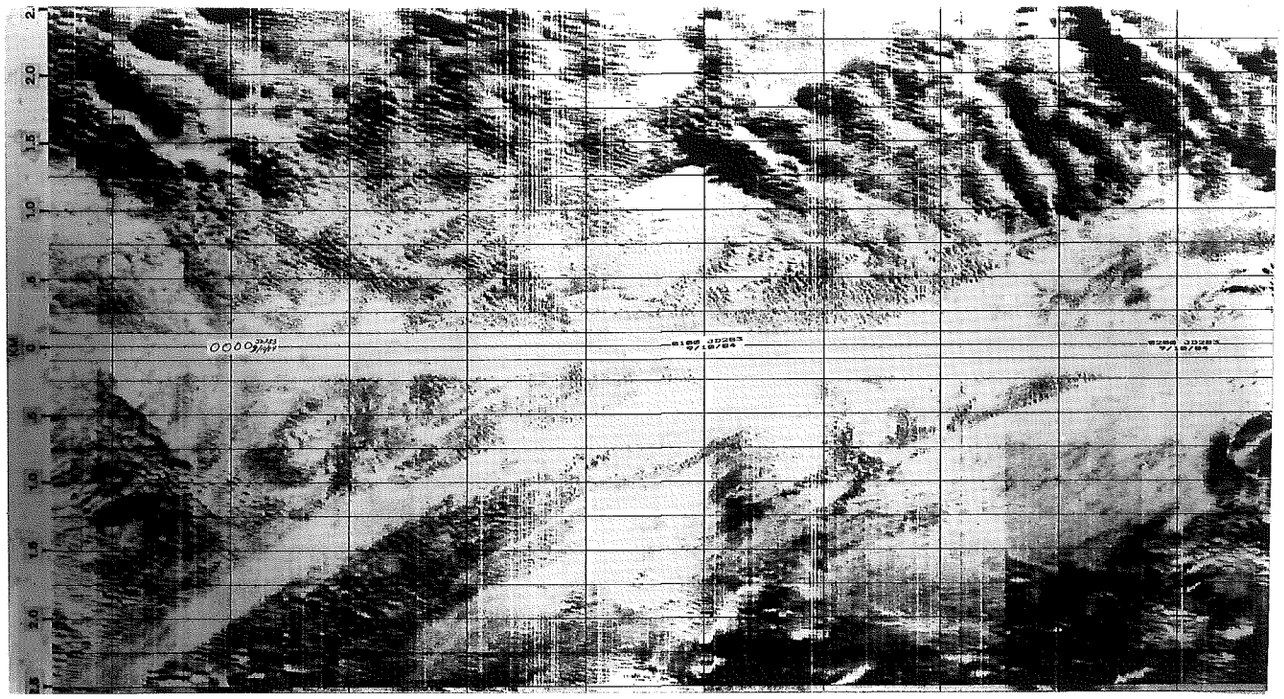

Figure 13a:

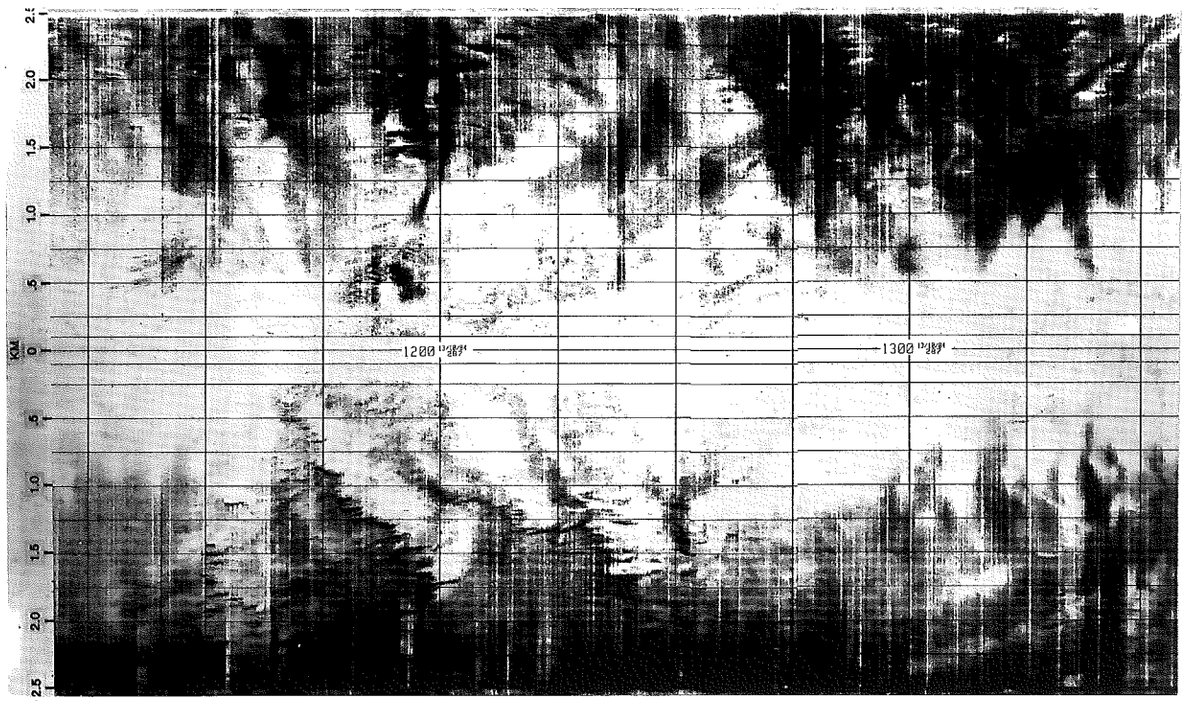

Figure 13b:

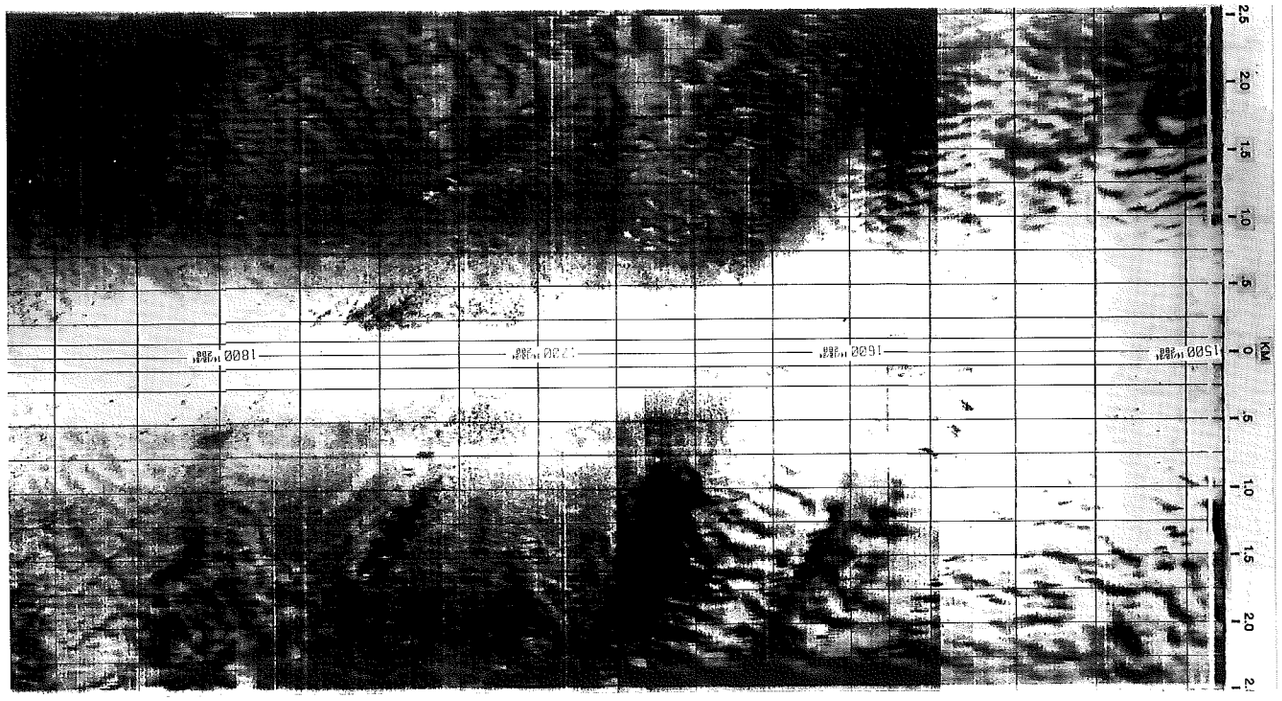

Figure 14a:

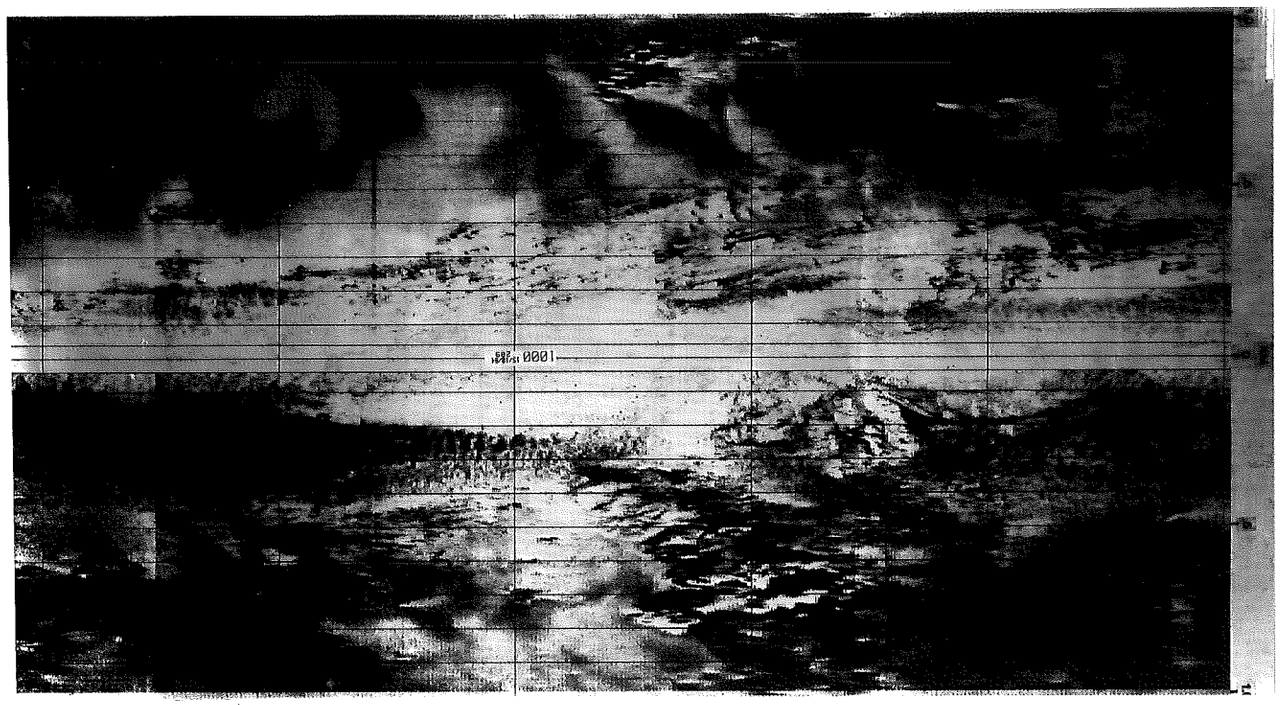

Figure 14b:

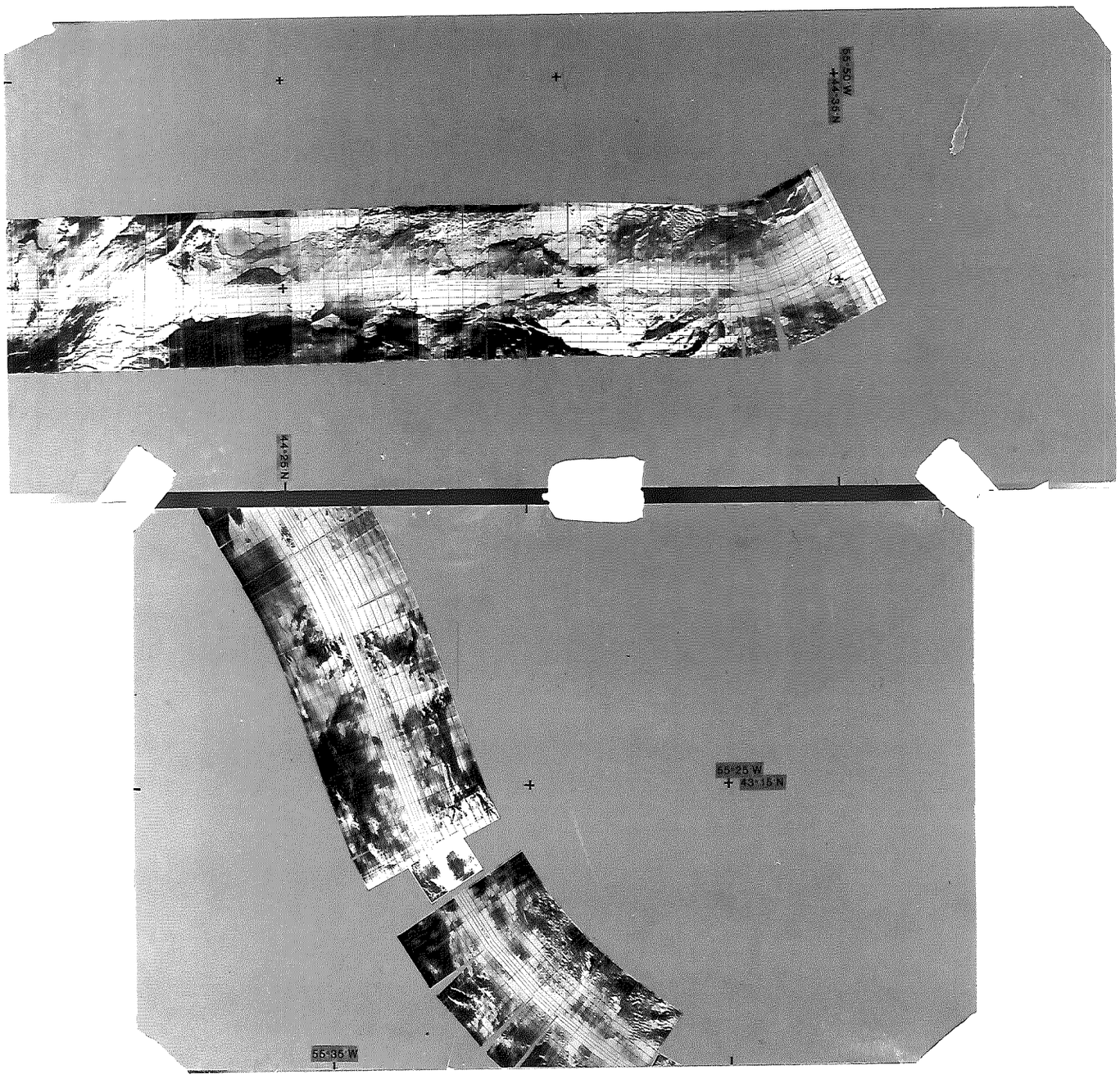

Plate I:

Plate V:

Plate II:

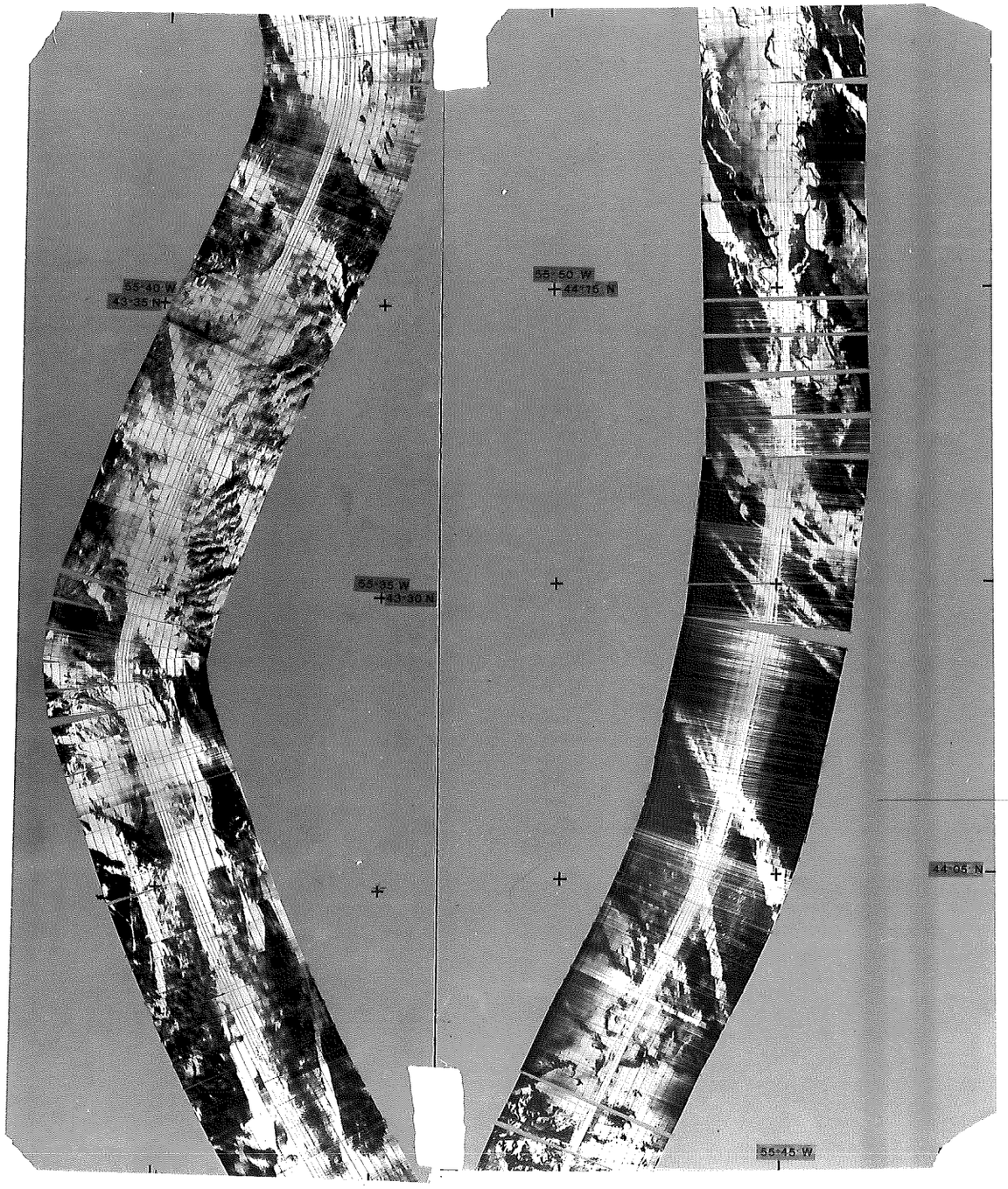

Plate IV:

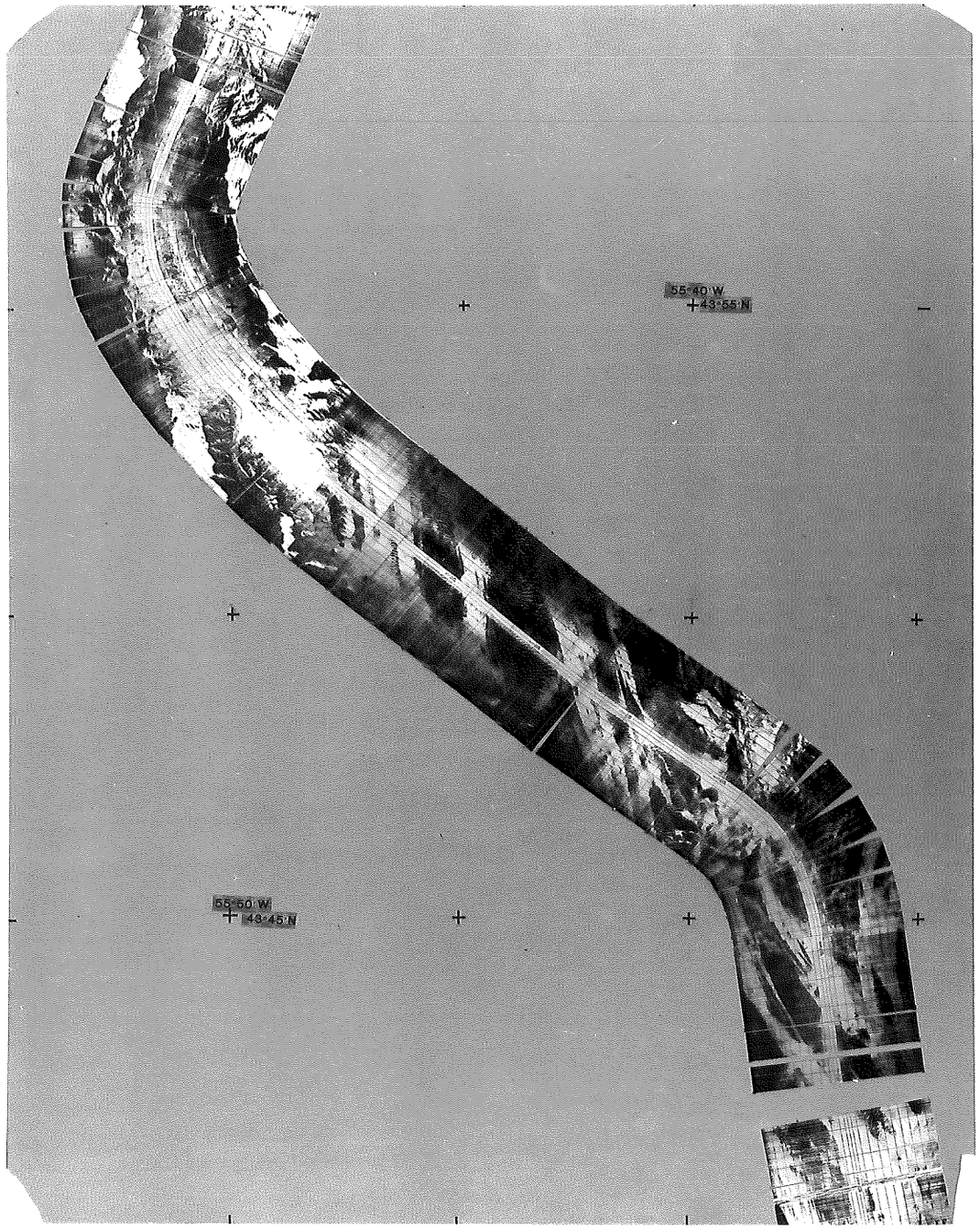

Plate III:

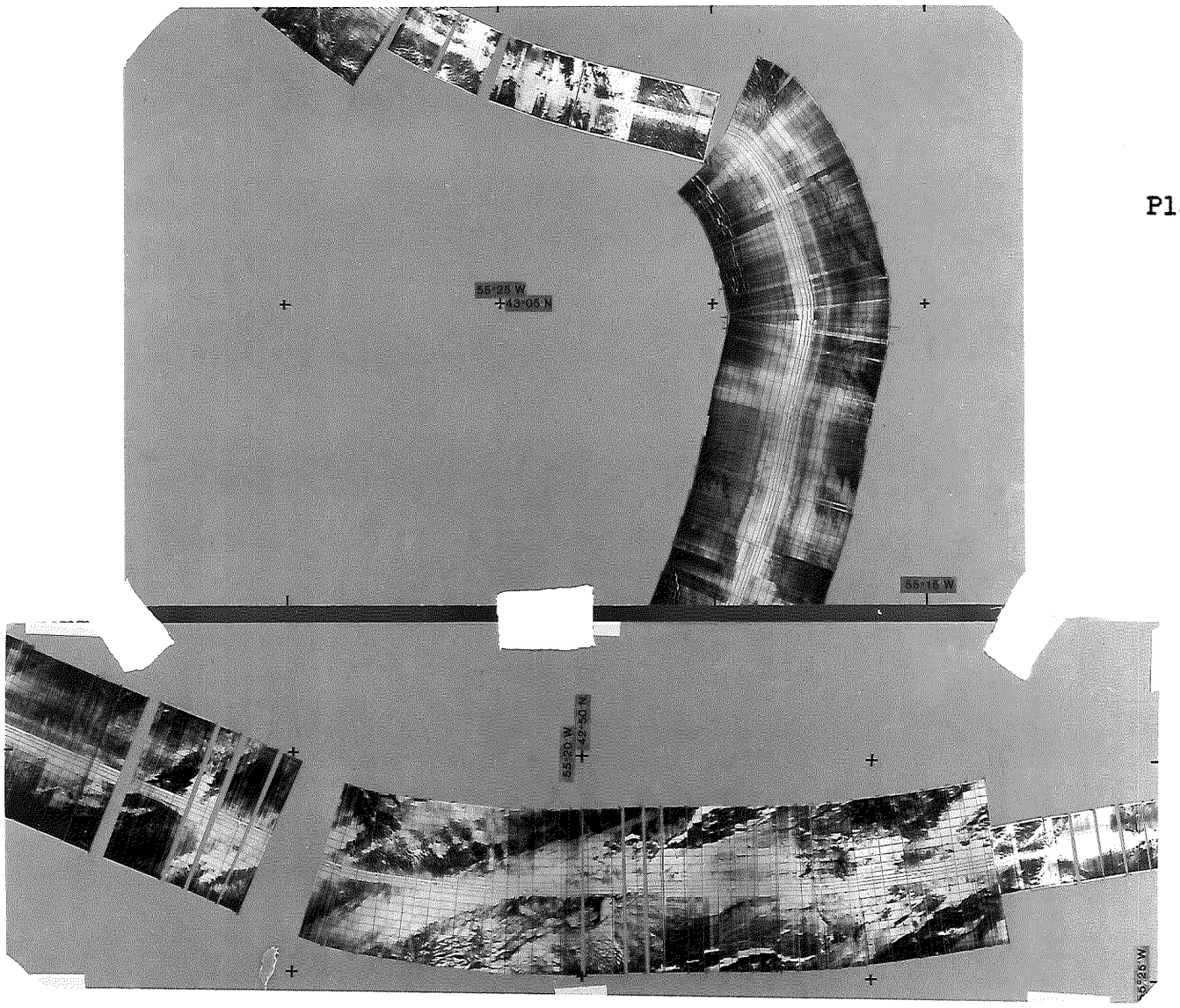

Plate VI:

Plate VII:

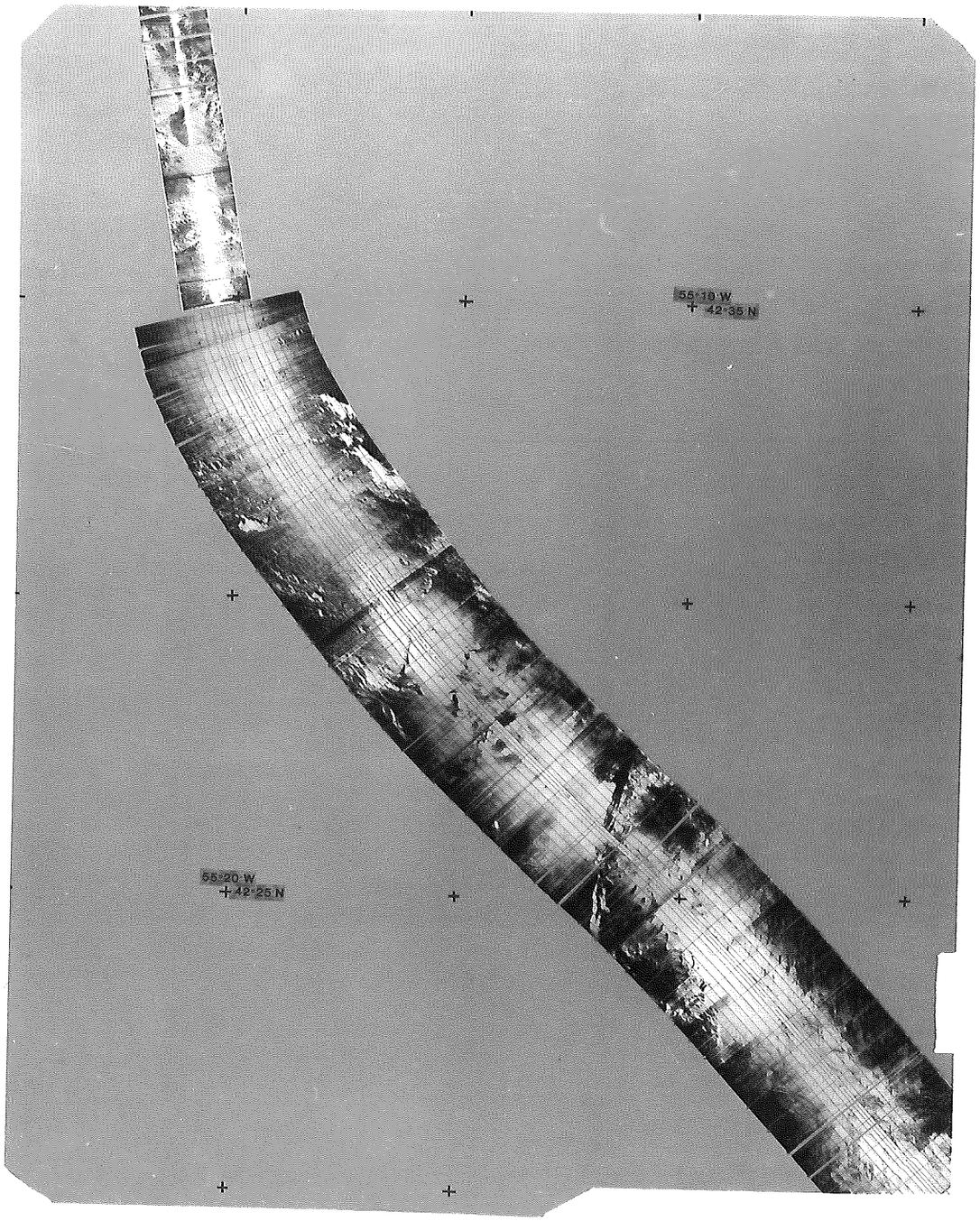

Plate VIII:

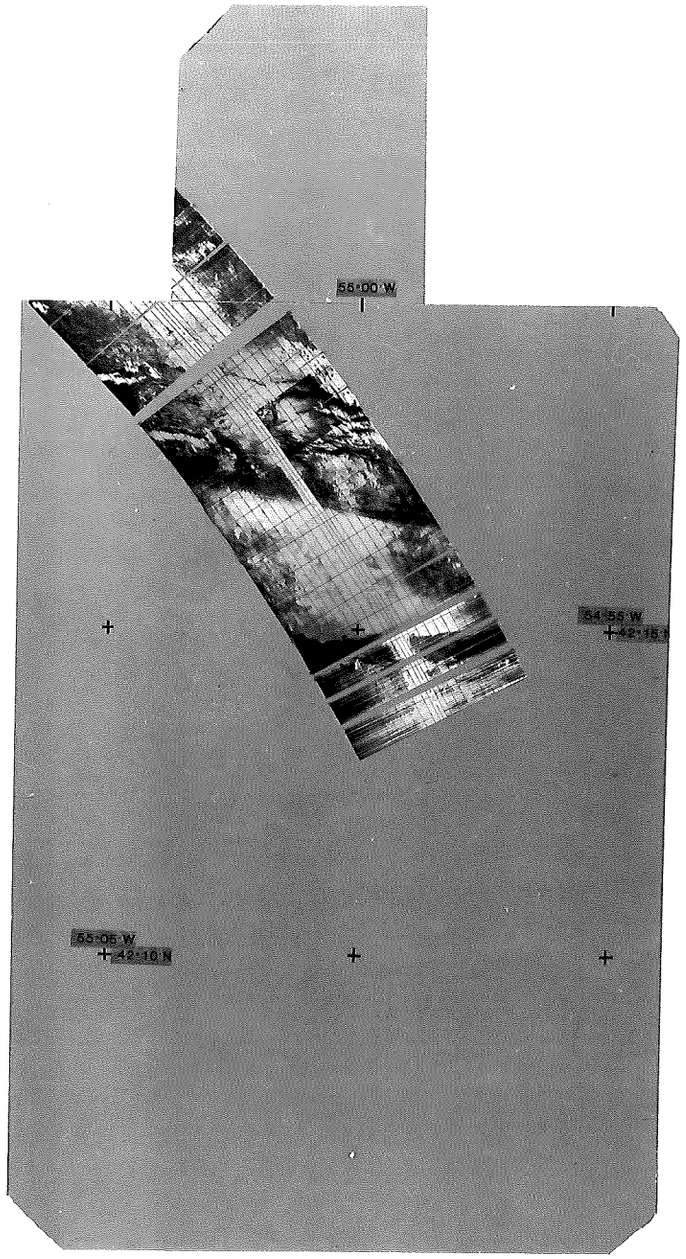

Plate IX:

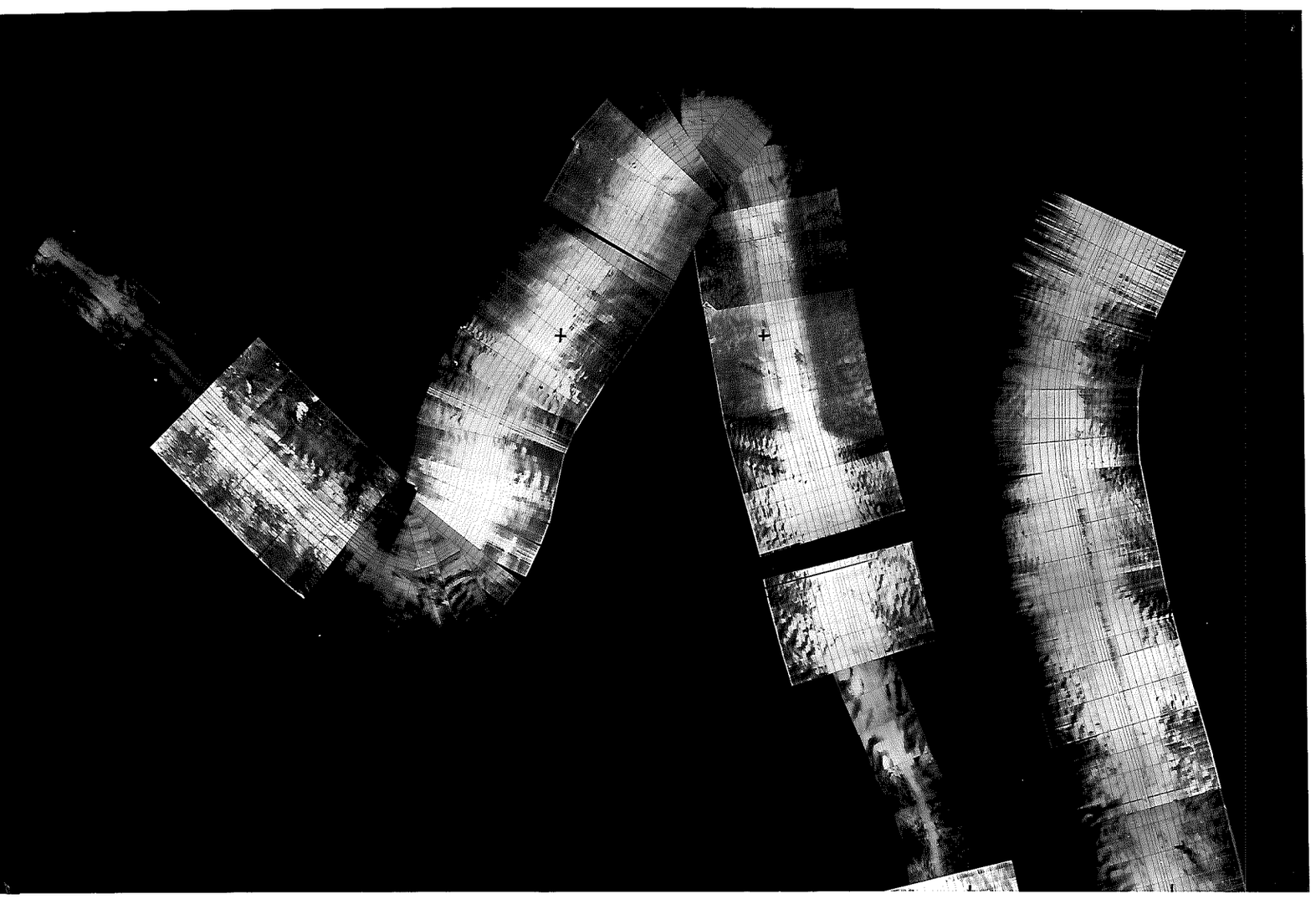

Hughes Clarke, 1987. Plate X: